

Glyco-Nanomaterials: Translating Insights from the “Sugar-Code” to Biomedical Applications

Kheireddine El-Boubbou and Xuefei Huang*

Department of Chemistry, Michigan State University, East Lansing, MI 48824, USA

Abstract: Over the past decade, diagnostics and therapeutics have changed gradually towards the use of more specific and targeted approaches. The most profound impact has been in the nanotechnology sectors, where an explosion in directing biomolecules to specific biomarkers has illustrated great potentials not only in detection but also in targeted therapy. Increased knowledge of the diseases at the molecular level catalyzed a shift towards identifying new biological indicators. In particular, carbohydrate-mediated molecular recognitions using nano-vehicles are likely to increasingly affect medicine opening a new area of biomedical applications. This article provides an overview of the recent progress made in recruiting the “sugar code” functionalized on various nano-platforms to decipher cellular information for both *in vitro* and *in vivo* applications. Today’s glyco-technologies are enabling better detection with great therapeutic potentials. Tomorrow they are likely to bring a full understanding of the “cell-glycananomaterial bio-conversation” where major biomedical problems will be overcome translating insights from the “glyco-nanoworld” into clinical practice.

Keywords: Magnetic glycananoparticles, magnetic resonance imaging, gold glycananoparticles, glyco-quantum dots, glyco-carbon nanotubes, glyco-nanomaterials, glyco-dendrimers, sugar code.

1. INTRODUCTION

During the last decade, there has been an explosion in the fabrication, characterization and applications of nanomaterials, which can potentially revolutionize the diagnosis and treatment of diseases [1-4]. Knowledge at the cellular and molecular levels has increased greatly, catalyzing a shift towards using more specific and targeted nano-therapies. With the recognition of the important multi-faceted roles carbohydrates play in many biological systems [5-7], tremendous advances have been made in recruiting sugar-functionalized nanocomposites for biological applications. Glyco-nanomaterials have attracted a great deal of attention owing to their carbohydrate functionality, small sizes, polyvalency, biocompatibility, as well as beneficial optical, electronic and magnetic properties. In this review, we will summarize the development of glyco-nanotechnology and their applications in sensing, imaging and therapeutic interventions [8-10].

2. THE “GLYCO” PERSPECTIVE

Signal transduction and appropriate communication between two cells are critical for cell growth and development. The bio-conversation between two cells involves a ligand from the sender and a receptor on the cell surface receiving the signal. Due to their rich structural variations, carbohydrates are uniquely suited for biological information transfer [5,11,12]. As one of the common cell-surface ligands, carbohydrates can direct the initiation of many medically important physiological processes where they are involved in a wide variety of events [13-16], including inflammatory and immunological responses [17-19], tumor metastasis [20], cell-cell signaling [21], apoptosis, adhesion [22], bacterial and viral recognition [22,23], and anticoagulation [24].

To realize the full potential of carbohydrates in diagnosis and therapeutic applications, several obstacles need to be overcome. The interaction between a single carbohydrate and its receptor is usually weak, typically with mM affinity. Nature solves this problem by simultaneously engaging multiple ligands for binding [25,26], leading to enhanced avidity through the multivalency effect [27]. Thus, a suitable platform is required to display carbohydrates in a polyvalent format in order to improve the binding strength and selectivity. The second challenge is that unlike the lock-and-key type of specific molecular recognition common in antigen and antibody binding [28], there can be several types of

receptors recognizing the same carbohydrate ligand. Strategies need to be developed to differentiate these receptors. The third challenge relates to the availability of pure carbohydrates for biological studies. It is difficult to purify large quantities of complex oligosaccharides from natural sources due to the heterogeneity of carbohydrates on cell surfaces and proteins. Although chemical and enzymatic synthesis of oligosaccharides and glyco-conjugates has undergone tremendous progress [29], it is still restricted to specialized laboratories. Therefore, the realization of full potential of carbohydrates in biomedical applications requires a multi-disciplinary approach bringing together glyco-biologists, materials chemists and synthetic chemists.

3. THE “NANO” PERSPECTIVE

At the nanometer dimension, materials often have novel optical, electronic, structural and surface properties as a consequence of their small sizes. Nanomaterials have attracted wide attention where extensive efforts have been devoted to methodological studies toward their synthesis, surface modification and biological applications [30-33]. Advances in nanoresearch have led to the development of novel nanoparticles (NPs) where size, geometry and surface functionality can be controlled at the nanoscale [34,35]. Diverse metal and semiconductor core materials have been used to construct nanomaterials with important physical and electronic properties ranging from high optical extinctions (gold) [2], surface-enhanced Raman effect (silver and gold) [36,37], stable photoemission (quantum dots) [38], and super-paramagnetism (iron oxide) [39]. When coupled to affinity ligands such as antibodies [40], proteins or peptides [41], oligonucleotides [42], or carbohydrates [43], nanomaterials are excellent vehicles for biological applications at the cellular and molecular level. However, several features need to be fine-tuned including ligand density, particle diameter, surface charges, magnetic, electronic or optical properties, stability, and targeting specificity.

Nanomaterials can serve as promising platforms for displaying carbohydrates for biological recognition. Due to the smaller sizes of NPs compared to their micrometer sized counterparts, NPs have much larger surface areas, which can enable higher capacity in receptor binding. In addition, multiple carbohydrate ligands can be immobilized onto one NP, which can potentially enhance the weak affinities of individual ligands to their binding partners. There are reports of many types of NPs bearing carbohydrates. Herein, we will focus on NPs functionalized with carbohydrates that play key roles in the molecular recognition processes rather than those where carbohydrates mainly function as NP stabilizing agents [44-47]. Furthermore, we will concentrate on several types of nanomaterials,

*Address correspondence to this author at the Department of Chemistry, Michigan State University, East Lansing, MI 48824, USA; Tel: (517) 355-9715, ext 329; Fax: (517) 353-1793; E-mail: xuefei@chemistry.msu.edu

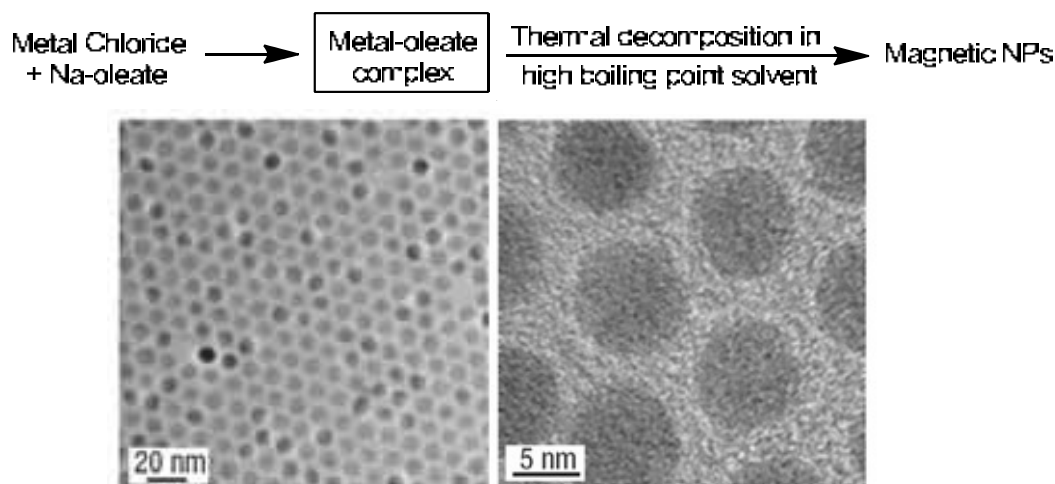


Fig. (1). Synthesis of highly crystalline monodispersed nanocrystals *via* thermal decomposition of metal-oleate complex; TEM images of 9 nm iron oxide nanocrystals [66]. (Copyright Nature Publishing Group. Reproduced with permission).

i.e., magnetic NP, gold NP, quantum dots, carbon nanotubes and dendrimers. In the following, we will divide our discussions according to the NP core composition and discuss the applications of each type of glyco-nanomaterial. In addition, as magnetic glyco-NPs and gold glyco-NPs have been extensively explored, sessions regarding their synthesis and fabrications are included.

4. MAGNETIC GLYCO-NP

Magnetic NPs are a class of NPs possessing magnetic moments when placed in an external magnetic field. The most used type of magnetic NPs is the Fe_3O_4 magnetite NPs. Some of the chief attributes of Fe_3O_4 NPs are: a) biocompatibility: these NPs are well tolerated by human bodies, as exemplified by the FDA approval of the usage of a type of magnetite NP, i.e., Feridex for liver imaging [48]; b) magnetic properties: the magnetite particles are highly magnetic in an external magnetic field, which can enable magnet induced separation thus facilitating biological purifications [49]. In addition, controlling the synthetic aspects can yield to magnetic NPs that respond rapidly to an applied magnetic field, but retain no magnetism once the external field is removed. This so called superparamagnetic attribute is important for preventing NP aggregation and ensuring colloidal stability. With their high magnetic relaxivities, the magnetic NPs can be used as contrast agents for Magnetic Resonance Imaging (MRI), which are useful for non-invasive label free biological detection both *in vitro* [50-52] and *in vivo* [40,41,53,54] applications; c) functionality: innovative methods are available to functionalize the NPs with a variety of biologically important molecules as carriers for immunoassay [42], biosensing [55], bioseparation [56] as well as drug delivery [53]. In this session, we will provide a general discussion on the synthesis of magnetic glyco-NPs followed by their *in vitro* and *in vivo* applications.

4.1. Synthesis of Magnetic Glyco-NPs

The magnetic NPs consist mainly of two parts: a) a magnetic $\text{Fe}_3\text{O}_4/\text{Fe}_2\text{O}_3$ core and b) a coating that functions to keep the metal oxides dispersed and colloidal through combined electrostatic and steric stabilization effects. Attention should be paid to the synthetic methods as they can significantly affect the size, shape, magnetic properties and hence the fate of nanocomposites in biomedical applications. Many chemical methods have been developed to synthesize such particles: co-precipitation, thermal decomposition, microemulsions, sol-gel syntheses, hydrothermal reactions, and spray pyrolysis [30,32]. Herein, we will focus on two most

extensively studied methods, i.e., co-precipitation and thermal decomposition.

4.1.1. Co-Precipitation Method

The co-precipitation technique is probably the simplest chemical pathway to obtain magnetic NPs with a good control in size, shape and uniformity. Iron oxides, either Fe_3O_4 or $\gamma\text{-Fe}_2\text{O}_3$, are usually prepared *via* the Massart method [57] by aging appropriate stoichiometric ratios of Fe^{2+} and Fe^{3+} salts in an aqueous basic media in the presence of stabilizing molecules.

The magnetic NPs produced through this procedure are spherical, and hydrophilic. According to the thermodynamics of this reaction, complete precipitation of Fe_3O_4 in the presence of a base should be expected at a pH ~8-14 with a stoichiometric ratio of ($\text{Fe}^{3+}/\text{Fe}^{2+}$ 2:1) under nitrogen. An increase of the mixing rate tends to decrease the particle size. A decrease of the size and polydispersity is also noted when the base is added to the salt mixture as compared to the opposite process. Moreover, the size is strongly dependent upon the acidity and the ionic strength of the precipitation medium. The higher the pH and ionic strength, the smaller the particle size and size distribution will be.

In an alkaline medium of pH > 8, polarizing or highly charged ions, such as ammonium or alkaline may give rise to flocculation (the process by which NPs clump together). The addition of chelating organic anions (i.e. carboxylate ions such as acrylic or oleic acid) or surface complexing polymers (e.g. dextran, polyglutamic acid (PGA), polyvinylpyrrolidone (PVP) or polyvinyl alcohol (PVA)) during the formation of magnetite can help control the distribution, size and stability of the NPs [35]. Magnetite NPs can also be stabilized with silica to form magnetic silica nanospheres with various functional groups such as amines and carboxylates on the surface [58-61]. The size of the particles can be controlled by changing the silica/iron oxide ratio [59]. Surface functionalization of magnetic NPs can not only protect and stabilize the core, but also improve biocompatibility and bestow targeting abilities [39,62].

4.1.2. Thermal-Decomposition Method

To improve the monodispersity and magnetic susceptibility of the magnetic NPs, high temperature thermal decomposition methods were developed. Heating a 1,2-hexadecanediol solution of iron(III) acetylacetonate ($\text{Fe}(\text{acac})_3$) in the presence of oleic acid and oleylamine from 200 – 300°C led to the formation of highly monodispersed magnetite Fe_3O_4 NPs [63]. Metal ferrites (MFe_2O_4 , where M=Co, Fe, Mn, etc.) were also synthesized in the form of

mono-dispersed cubic and spherical NPs by the seed-mediated growth process using $\text{Fe}(\text{acac})_3$ and $\text{M}(\text{acac})_2$ as reactants [64]. The superparamagnetic maghemite $\gamma\text{-Fe}_2\text{O}_3$ nanocrystals were prepared *via* high-temperature aging of iron-oleic metal complex using iron pentacarbonyl ($\text{Fe}(\text{CO})_5$) in the presence of oleic acid at 100 °C [65]. This synthesis could be scaled up in an ultra-large-scale synthesis *via* thermal decomposition of metal-oleate precursors in high boiling solvent (benzyl ether) with high yield, uniformity, good crystallinity and reproducibility (Fig. 1) [66].

The high-temperature thermolysis procedures produce nanocrystals with hydrophobic surfaces and hence only dispersible in nonpolar organic solvents. For biological applications, it is of great importance to find an effective approach to make them fully dispersible in aqueous media. One popular method is through “ligand-exchange” [67], where the hydrophobic ligands on the particle surface are replaced by molecules containing polar groups. Another method is to use amphiphilic [41] or tri-block polymers [38], which bear hydrophobic chains and hydrophilic head groups. The hydrophobic groups anchor the polymer onto the surface of the nanocrystals, while the hydrophilic head groups render the coated nanocrystals freely soluble in aqueous media.

4.1.3. Immobilization of Carbohydrates onto Magnetic NPs

In order to attach carbohydrates onto magnetic NPs, the most direct method is through *in situ* immobilization using carbohydrates as the stabilizing agent during formation of the NPs (Fig. 2a) [68,69]. For example, dextran has been used to directly coat magnetite as in Feridex preparation [69]. However, the *in situ* immobilization typically requires a large amount of carbohydrates and it is most effective for polysaccharide coating as chelation of mono- and oligo-saccharides to the NP surface may reduce the number of available functional groups for biological recognition.

An alternative to the *in situ* immobilization procedure is the post-synthetic functionalization approach by attaching carbohydrates to pre-fabricated NPs (Fig. 2b). This can be accomplished by functionalizing magnetic nanospheres with amines, on which carbohydrates can be covalently linked either through amidation [70,71] or chemoselective formation of amidines [43]. Carbohydrates can also be attached using the highly selective [3+2] Huisgen cycloaddition reaction (Fig. 2c) [72-74]. It was reported that the alkyne derivatized carbohydrate reacting with azide functionalized NPs gave better conjugate efficiency compared to that using alkynated NPs with azide bearing molecules [74]. In addition, the high affinity binding between streptavidin and biotin can be utilized by incubating biotinated carbohydrates with streptavidin coated NPs [75,76].

The aforementioned post-synthetic modification procedures require covalent functionalization of carbohydrates with a reactive group prior to NP conjugation. A new approach to introduce unmodified carbohydrates is through photochemically initiated coupling between perfluorophenyl azide functionalized magnetic NPs and carbohydrates (Fig. 2d) [77]. Upon light activation, the NP surface azide moieties can be converted to highly reactive nitrenes, which insert into CH or NH bonds on carbohydrates allowing their covalent attachment without the need to derivatize the carbohydrates.

4.2. *In Vitro* Biological Applications of Magnetic Glyco-NPs

4.2.1. Lectin Interactions

It is crucial that upon carbohydrate immobilization onto magnetic NPs, their biological recognitions are retained. We explored this using plant lectins, which are non-enzyme

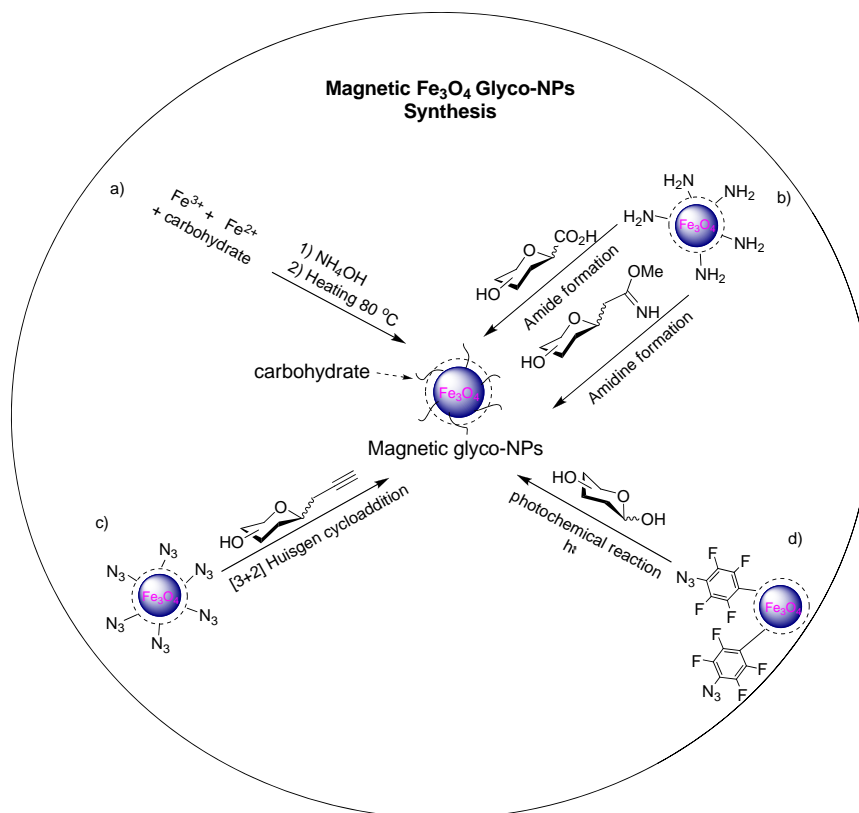


Fig. (2). Schematic demonstration of common methods for synthesis of magnetic glyco-NPs.

carbohydrate binding proteins [72]. Upon incubation with a fluorescently labeled lectin, if the magnetic glyco-NPs (MGNPs) can bind with the lectin, subsequent application of an external magnetic field to the sample should remove the lectin from the solution leading to a reduction of fluorescent intensity of the supernatant. Concanavalin A (Con A) is a well characterized mannose (Man) selective lectin with weak galactose (Gal) binding affinities [78]. Incubation of Man functionalized MGNP with fluorescein isocyanate (FITC) labeled Con A followed by magnetic separation led to a 89% reduction in fluorescent intensity of the solution, while the same amount of the weakly bound Gal-MGNP was able to remove only 8% of the Con A (Fig. 3). This is consistent with the known carbohydrate binding preferences of Con A [78]. High concentration of free mannose (2500 times the amount of Man on the NPs) was required to partially disrupt the Con A/Man-MGNP complex. This suggests that the avidity of Man-MGNP to Con A was three orders of magnitude higher than the affinity of the monomeric mannose on per sugar basis, which highlight the advantage of multivalent appeal of MGNP with ligand clustering leading to strong binding.

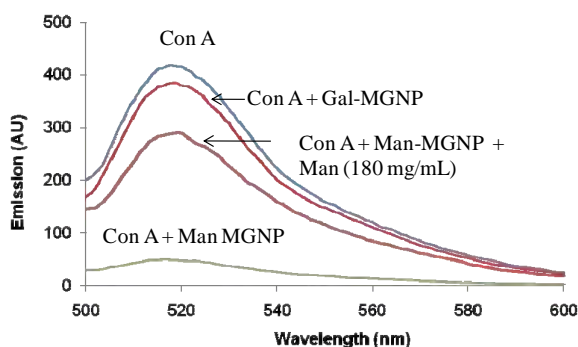


Fig. (3). Fluorescent emission intensities of supernatants of FITC-Con A (100 microgram/mL) upon incubation with various MGNPs (1 mg/mL, ~0.08 mg/mL carbohydrate) followed by magnet mediated separation ($\lambda_{\text{excitation}} = 494 \text{ nm}$) [72]. (Copyright American Chemical Society. Reproduced with permission).

4.2.2. Bacterium Detection

As bacterium infections present a significant threat to public health, simple and rapid methods for pathogen detection and removal are urgently needed to quantify the risks of contamination and help reduce potential infections. Many pathogens initiate the infections through the binding of extracellular lectins with host cells glycoalyx [79,80]. The understanding of such adhesion phenomena, at both the cellular and molecular levels, presents a promising approach to fight against pathogens in the era of increasing antibiotic resistance [81].

The Gram negative *Escherichia coli* (*E. coli*) was commonly used as a model pathogen and it is known that *E. coli* strains such as ORN178 contain mannose binding protein FimH in their pili [82]. To detect *E. coli*, we synthesized magnetite NPs functionalized with Man [73]. Our *E. coli* detection assay involved incubation of the functionalized Man-MGNPs with *E. coli* for a few minutes, followed by treatment with a hand-held magnet (Fig. 4). The magnetic nature of the NPs enabled rapid magnet mediated separation. With just five minute incubation, 65% of the *E. coli* ORN178 cells were removed from the solution with a capture efficiency up to 88% after 45 minute incubation. This assay was fast and simple with a detection limit of 10^4 cells/mL. A challenge in using carbohydrates for pathogen detection is that different types of bacteria may bind with the same carbohydrate albeit with various affinities. To address this issue, in addition to Man-MGNPs, we prepared MGNPs containing Gal on the surface. Based on the response patterns to Gal-MGNPs and Man-MGNPs, three different *E. coli* strains (ORN178, ORN208, and an environmental strain) were easily differentiated highlighting the potential of MGNPs in bio-sensing. Thus, MGNPs presented a unique approach, which can be used not only for rapid pathogen detection, but also for strain differentiation and efficient pathogen decontamination.

Yan and coworkers prepared Man-functionalized iron oxide NPs via photochemically activated phosphate perfluorophenylazides (PFPA) coupling chemistry [77]. Although a potential concern of this method is the alteration of carbohydrate structures by the photochemical reactions, it was demonstrated that their Man-MGNPs retained the expected recognition by Con A. Upon incubation with the mannose binding *E. coli* strain ORN178, the NPs were selectively attached to *E. coli* as visualized by TEM (Fig. 5).

Instead of using NPs, Iyer and coworkers immobilized biotinylated Man on magnetic microparticles to capture and detect *E. coli* through a luminescent assay [76]. Capture efficiencies of 20 - 35 % for *E. coli* ORN 178 were observed with these Man microparticles [76], which was lower than those using MGNPs [73]. This is presumably due to the larger surface areas of MGNPs compared to their micrometer sized counterparts allowing more efficient magnetization of bacteria, which highlights the advantages of using NPs. In addition, this study provided a head to head comparison between synthetic glyco-conjugates and antibodies for *E. coli* detection. They observed that the glyco-beads were better than their antibody-counterparts in both sensitivity and selectivity, as only ~ 5 - 15 % capture efficiencies for *E. coli* ORN 178 were achieved using antibody beads. This is likely due to the smaller size of the glycoconjugate resulting in better packing density on *E. coli* and thus tighter binding. Although more examples are needed to demonstrate the generality of these observations, this study underscored the potential of using glycoconjugate-based high affinity reagents for biosensing.

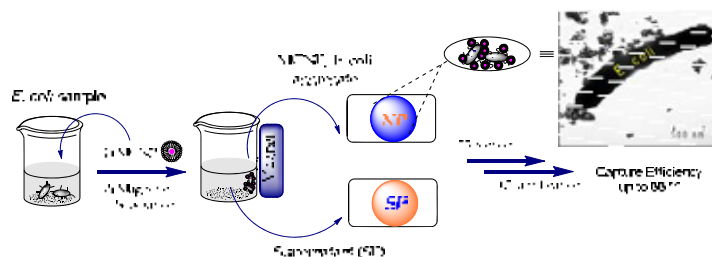


Fig. (4). Incubation of *E. coli* strain ORN178 and Man-MGNPs followed by magnet mediated separation detected the presence of bacteria with up to 88% of the bacteria removed by this procedure.

Bacterium detection was not just limited to *E. coli*. Pieters and coworkers detected the gram-positive pathogenic *Streptococcus suis* bacteria known to bind to galabiose (Gal- α 1,4-Gal) using biotinylated sugars coated on streptavidin bearing magnetic particles [75]. Through a luminescence assay that quantified the bacterial ATP, monovalent and tetravalent galabioside-functionalized particles yielded strong signals with a detection limit of 10^4 bacteria/mL, whereas N-acetylglucosamine (GlcNAc) coated particles did not bind indicating the galabiose recognition specificity. Importantly, experiments with larger magnetic particles (diameter ~ 10 nm) did not enable successful bacterial detection, which provided additional evidence on the importance of large surface area resulting from the usage of glyco-NPs.

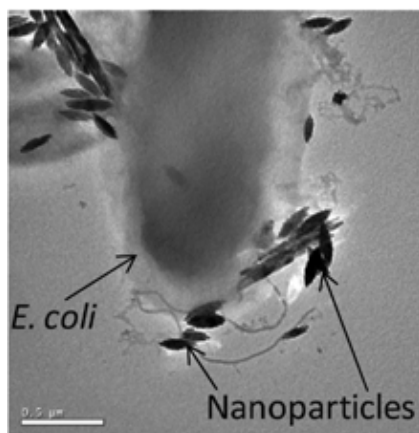


Fig. (5). TEM images of *E. coli* ORN178 strain after treating with Man-functionalized hematite iron oxide NPs [77] (Copyright American Chemical Society. Reproduced with permission).

4.2.3. Cancer Cell Binding

The Park group reported the fabrication of highly colloidal hyaluronic acid (HA), a naturally existing polysaccharide, coated superparamagnetic iron oxide nanocrystals (~ 15.2 nm diameter) as target-specific MR imaging probes [83]. Cancer cells often express HA receptors such as CD44 [84]. Park and coworkers demonstrated that the uptake of the HA-NPs by human colon carcinoma HCT116 cells overexpressing CD44 was enhanced compared to the NIH3T3 fibroblast cells, which expressed little CD44. MR imaging revealed that upon HA-NP incubation, the contrast change of HCT116 cells was four fold that of NIH3T3 cells (Fig. 6). Incubation of free HA reduced the MR contrast of the HA-NP/HCT116 more than that from HA-NP/NIH3T3 cells supporting the role HA played in HCT116 cellular uptake of the NPs. The Mohapatra group described the synthesis of HA-Fe₂O₃ hybrid nanocomposites

(average diameters < 160 nm) via electrostatic interactions of oil-in-water HA nanoemulsion and Fe₂O₃ NPs [85]. They showed these NPs were effective in delivering encapsulated atrial natriuretic peptides to the nuclei of human lung adenocarcinoma cell A549 and human kidney cell HEK293 over-expressing CD44. Nuclear targeting was also observed by our group in studying HA-NP interactions with macrophages [86].

The successful detection and differentiation of *E. coli* using MGNPs prompted us to explore the possibility of cancer detection [72]. The development of simple and effective nanoprobes to detect and profile cancer cells can have great potential impacts on cancer research. Thus, we prepared a small library of MGNPs functionalized with different monosaccharides (Man, Gal, fucose (Fuc), sialic acid (Sia) and GlcNAc) and embarked to systematically profile and quantify a variety of cancer cells via MRI. We examined nine different types of cancer cells together with one normal cell line and explored whether we could distinguish all these cell lines. Although multiple cell types can bind the same carbohydrate, the differentiation of all ten cell lines was achieved through a statistic method, linear discriminant analysis (LDA) [87], based on different response patterns (ΔT_2 changes) of cells to the five types of MGNPs (Fig. 7). Through this approach, closely related isogenic tumor cells, cells with different metastatic potential and malignant vs normal cells were readily distinguished without prior knowledge on endogenous carbohydrate receptors. Moreover, MGNPs could significantly reduce the binding of tumor cells to the matrix, presenting a new method for anti-adhesive therapy studies of tumor. The ability to characterize and unlock the glyco-code of individual cell lines can thus facilitate both the understanding of the roles carbohydrates play in tumor development as well as the expansion of diagnostic and therapeutic tools for cancer detection via MRI. The LDA may be a general method to decipher the identities of cells/receptors where multiple types of cells/receptors can recognize the same carbohydrate ligand.

4.2.4. Stem Cell Monitoring

Mesenchymal stem cells (MSCs) have shown great potential in tissue engineering. It is important to be able to track stem cells non-invasively by MRI for investigating cell-tissue interactions and guiding the development of effective stem cell therapies [88,89]. In order to accomplish this, MRI contrast agents will need to be loaded into stem cells. Commercial magnetic NPs such as Feridex or Endorem (~ 100 - 150 nm), Resovist (~ 60 nm) and Sinerem (~ 20 - 40 nm) complexed with polycationic transfection agents especially poly-L-lysine (PLL) have been used for stem cell labeling [90,91]. However, due to the toxicity of transfection agents, it is desirable to explore other more biocompatible alternatives.

Syková *et al.* showed that mannose-modified iron oxide NPs (diameter ~ 60 - 70 nm) were efficient probes for labeling stem cells

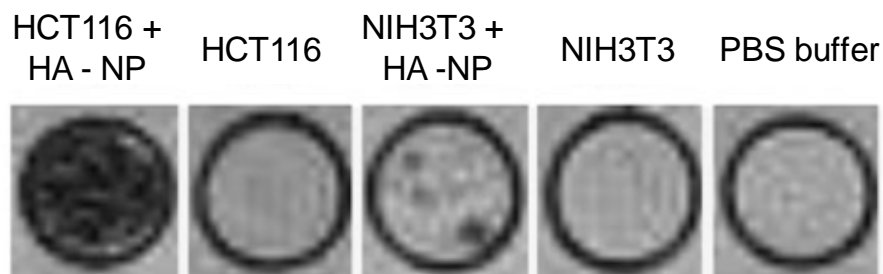


Fig. (6). T2 weighted MR images for CD44⁺ HCT116 cells and CD44⁻ NIH3T3 cells upon incubation of HA-NPs. (The image of HCT116 + HA-NP was four times darker than that of NIH3T3 + HA-NP based on T2 quantification) [83] (Copyright Wiley-VCH Verlag GmbH & Co. KGaA. Reproduced with permission).

[68]. They explored two procedures for NP fabrication, labeling with Man during or post NP synthesis. The NPs coated with Man post-synthetically were found to be more efficacious for cell labeling. These NPs crossed the cell membranes and were internalized well by rat bone marrow stromal (rMSCs) cells as visualized by Prussian blue staining and TEM. Compared with Endorem, lower concentrations of Man-NPs were needed and higher cellular uptake was achieved, which could be due to the presence of Man receptor on the cell surface.

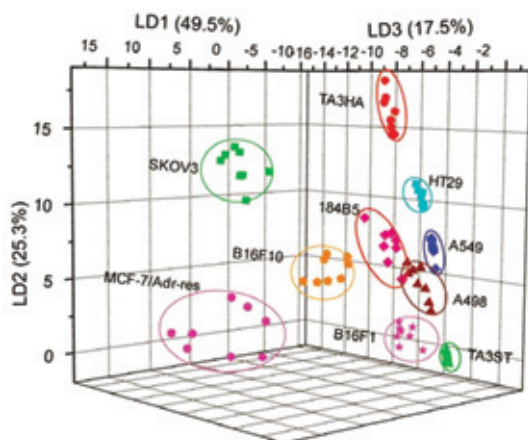


Fig. (7). LDA plot for the first three linear discriminants (LDs) of $\Delta T2$ patterns obtained with the MGNP array upon binding with 10 cell lines. Full differentiation of the 10 cell lines were achieved despite the simple structures of monosaccharide employed and the fact that different cell types can bind with the same carbohydrate [72]. (Copyright American Chemical Society. Reproduced with permission).

In addition to Man, superparamagnetic iron oxide NPs have been coated with (carboxymethyl)-chitosan for MR imaging of stem cells [70]. These particles were internalized into human MSCs (hMSCs) through endocytosis. Cell viability assays indicated that these particles were biocompatible and did not affect osteogenic and adipogenic differentiations of the cells. The *in vitro* detection threshold of cells was estimated to be about 40 cells. Results from these studies indicated that the biocompatible carbohydrate coated NPs show promise for use with MRI in visualizing hMSCs. Further studies are necessary to demonstrate its applicability to *in vivo* stem cell tracking.

4.3. *In Vivo* Applications of Magnetic Glyco-NPs

The Cho group prepared superparamagnetic MGNPs coated with a galactose polymer (Gal-SPIONs) (diameter \sim 25 nm) [92]. It is known that liver cell hepatocytes contain the galactoside binding

asialoglycoprotein receptor (ASGP-R) with galactose and galactosamine known to accumulate selectively in the liver *via* ASGP-R binding [93]. Confocal microscopy studies showed time-dependent uptake of these NPs into the cell membrane and cytosol of hepatocytes suggesting a receptor-mediated endocytosis [92]. Tail vein injection of these particles into rats exhibited a 75% $T2$ signal drop for rat liver by MRI, which was more than two times the contrast change (36%) observed using control NPs without any galactose (Fig. 8). In a separate study by the same group, NPs bearing mannan were fabricated [94]. The mannan not only protected the NPs from aggregating in physiological medium but also enhanced NP delivery to liver presumably through binding mannose receptor on liver macrophages for MRI. These results suggest the potential utility of MGNPs as liver-targeting MRI contrast agent.

Davis and coworkers demonstrated the utility of glycan sialyl Lewis^x (sLe^x) functionalized iron oxide coated-NP (sLe^x-NP) (average mean size \sim 86 nm) to specifically target CD62 [43]. The carbohydrate-binding transmembrane proteins CD62E (E-selectin) and CD62P (P-selectin) are important in recruiting leukocytes to sites of inflammation and are up-regulated on the activated brain endothelium in response to injury [95]. Specific visualization of the early-activated cerebral endothelium using magnetic NPs provides a new tool for the pre-symptomatic diagnosis of brain disease and evaluation of new therapies. To this end, selectin expression on activated endothelium in the brain was induced by microinjection of interleukin-1 β followed by the systematic injection of sLe^x-NP (4 mg Fe/kg) in a rat model. Direct targeted detection of endothelial markers E/P selectin (CD62E/CD62P) in acute inflammation was achieved *via* MRI (Fig. 9). This raises exciting opportunities to use suitably designed glyco-NPs for early detection of neurological diseases.

5. GOLD GLYCO-NPs

5.1. Gold-NP Synthesis

Gold (Au) nanocomposites, including nanospheres, nanorods, and nanoshells (size \sim 10 to 100 nm) have unique optical properties. Due to the strong plasmon resonance, absorption and scattering of electromagnetic radiation by such nanocomposites are strongly enhanced [96]. The magnitudes of light scattering and absorption by gold nano-materials can be orders of magnitude higher than those from traditional fluorescence dyes [36,97].

The optical properties of the gold nanocomposites are highly dependent upon their diameter, shape and aspect ratio. By changing the aspect ratio as well as the structure of nanocomposites [2,36], the maximum extinction wavelength can be tuned from the visible to near-infrared region (NIR) (650–900 nm), where tissue absorption in NIR window is minimal. The unique optical properties coupled with their straightforward simple synthesis and exceptional stability have rendered Au-NPs well suited for applications in imaging, sensing, biology and medicine [36,37,98].

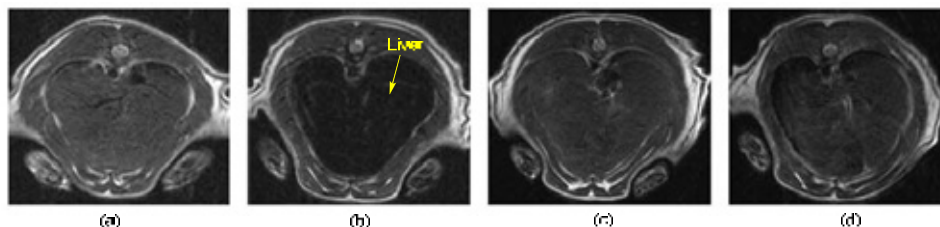


Fig. (8). $T2$ -weighted MR image (a) preinjection and (b) after 1-hour injection of Gal coated SPIONs; (c) pre- and (d) post-injection of control SPIONs without any carbohydrate coating. Significant signal drop (darkening) of liver was observed with the Gal-SPIONs compared to control NPs [92].

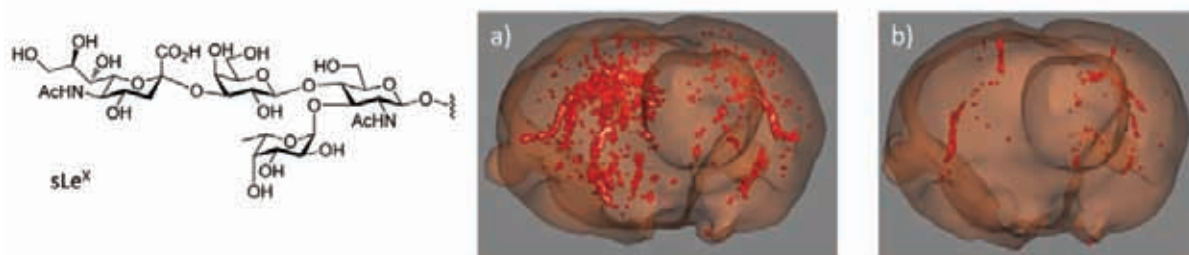


Fig. (9). Structure of sLe^x tetrasaccharide. 3D reconstruction of T2* weighted images of the brain of rats in a multiple sclerosis model. Rats were injected with **a**) sLe^x -NPs and **b**) the control NPs without sLe^x . The images showed that sLe^x -NPs enabled clear detection of the lesions [43]. (Copyright National Academy of Sciences. Reproduced with permission).

Although the synthesis of Au-NPs could be dated back to 1857 by Faraday [99], deeper insights into the fabrication of colloidal gold nanomaterials with controlled sizes, shapes and properties emerged only recently. Generally, reduction of metal salts such as auric acid ($H AuCl_4$) in aqueous media produces neutral Au atoms that gradually start to precipitate forming nanometer spherical particles upon vigorous stirring. Surfactants or chelating agents have been utilized as surface stabilizers and/or templates to control the synthesis. When bound to the NP surface, such molecules can not only decrease the surface energy and control the growth and shape of the particles, but also act as a stabilizer against aggregation.

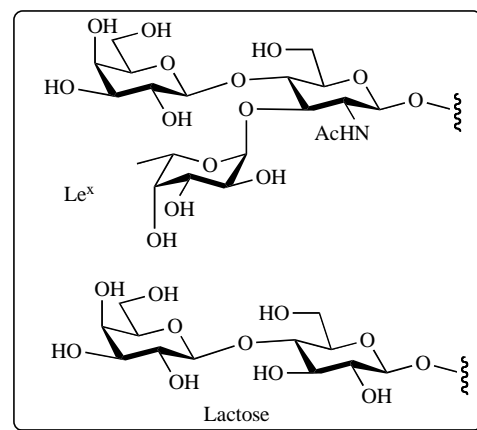
Here, the most commonly employed techniques for the fabrication of Au-NPs will be discussed. Detailed mechanistic insights and controlled-synthetic methodologies of gold nanomaterials can be found in details in several excellent reviews [100-102]. A simple method to synthesize gold nanospheres involves the reduction of $H AuCl_4$ by citrate to produce spheres with a relatively broad size range (diameters ~ 10 to 150 nm) and low monodispersity (especially for > 30 nm particles) [103-105]. Another widely known approach is to transfer gold ions to an organic phase mediated by a phase transfer catalyst tetraoctylammonium bromide (TOAB), followed by reduction with a strong reducing agent such as $NaBH_4$, which yield ~ 2 -5 nm Au-NPs [106]. To prevent aggregation, a stronger binding agent, usually a thiol ligand, is added that strongly binds gold surface. To better control size of the NPs, a powerful methodology, known as seed-mediated growth, has been developed. Briefly, gold ions are reduced by strong reducing agents to form seeds, i.e. small particles that are then used in the next growth step [107]. In the second stage, the reducing agent is generally mild [108], reducing only the precursor ions which are adsorbed onto the seed surface without creating any new nucleation center.

In order to fabricate gold glyco-NPs, three major approaches were developed. The most popular method involves the usage of thiol terminated carbohydrates as capping ligands during formation of Au-NPs [109-114]. This method is very convenient as carbohydrates can be readily functionalized with thiols usually at the reducing end. However, one drawback is the size of the particles obtained can vary significantly depending on the structure of the ligand as well as experimental conditions, which can be difficult to predict and control [115]. As an alternative, a post-synthetic ligand exchange procedure was developed [116-120]. Au-NPs were prepared first coated with a ligand such as CTAB, which would reproducibly generate Au-NPs with predictable sizes. The surface ligands on these NPs can then be exchanged with thiol terminated carbohydrates, leading to gold glyco-NPs. The third method involves *in situ* coating during formation of the NPs [121,122]. Carbohydrates bearing a free hemiacetal reducing end can function as mild reducing agents, reducing gold salt to form nanoparticles. The multiple hydroxyl groups in the carbohydrates can chelate with the gold surface providing a water soluble coating.

5.2. *In Vitro* Applications of Gold Glyco-NPs

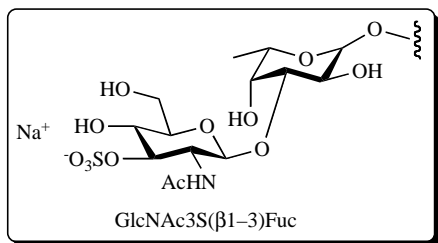
5.2.1. Studying Carbohydrate-Carbohydrate Interactions

Gold glyco-NPs have been successfully employed for studying carbohydrate-carbohydrate interactions. Penadés and coworkers did elegant work in this field where they prepared carbohydrate-functionalized Au-NPs to investigate carbohydrate-carbohydrate interactions and carbohydrate-mediated cell-cell adhesion processes. In an early report, they demonstrated the use of either disaccharide lactose (Lacto-) or trisaccharide Lewis^x (Le^x -) coated AuNPs multivalent ligand carriers for studying Ca^{2+} -mediated carbohydrate-carbohydrate interactions [114]. Le^x or lactose was functionalized with an alkylthiol at the reducing end, and the corresponding Au-NPs were prepared by reducing $H AuCl_4$ with $NaBH_4$ in presence of the glyco-thiols. Using TEM, it was revealed that only specific binding between Ca^{2+} and Le^x -AuNPs result in self-aggregation, while Lacto-AuNPs did not show any clustering proving the importance of sugar structure in inducing aggregation. This phenomenon was also confirmed by an atomic force microscopy (AFM) study of adhesion forces between Le^x antigens self-assembled on gold surfaces [123]. Furthermore, the kinetics and thermodynamics of carbohydrate-carbohydrate interactions were established by surface plasmon resonance (SPR) and isothermal titration calorimetry (ITC) [124,125]. Their results showed that Ca^{2+} -mediated aggregation of Le^x -AuNPs was a slow but highly exothermic process, while the heat evolved in the case of Lacto-AuNPs was very low and its thermal equilibrium was quickly achieved. Measurements in the presence of Mg^{2+} and Na^+ cations did not induce significant aggregation of Le^x -AuNPs confirming the requirement of Ca^{2+} for carbohydrate and carbohydrate interactions.



In another report, the Kamerling group demonstrated the chief role carbohydrates played in self-aggregation of the marine sponge *Microciona prolifera* using gold glyco-NPs [126]. It is known that cell aggregation in the *Microciona prolifera* is mediated by the proteoglycan-like macromolecular aggregation factor (MAF),

which carries polysaccharides with repeating disaccharide units of 3-*O* sulfated GlcNAc β 1–3 linked with a L-fucosyl unit (GlcNAc3S(β 1–3)Fuc). Kamerling and coworkers grafted the GlcNAc3S(β 1–3)Fuc disaccharide as well as several structural analogs of the disaccharide on AuNPs. Microscopic studies revealed that the stereochemistry of the glycosyl linkage, hydrophobic groups on the sugar moiety, the linker type and the presence of Ca^{2+} were crucial for carbohydrate-carbohydrate recognition.



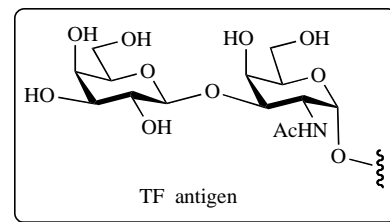
5.2.2. Carbohydrate-Protein and Carbohydrate-Antibody Interactions

Lin and coworkers used SPR to quantitatively analyze the binding affinity of the polyvalent glyco-NPs (Man-, Glc-, or Gal-AuNPs) with the lectin Con A [127]. The dissociation constant K_d of Man-Au NPs with Con A was determined to be 2.3 nM, representing a binding affinity over 5 orders of magnitude higher than that of the monomeric mannose. Furthermore, the change in avidity of different gold glyco-NPs with Con A followed the trend of their respective monovalent ligands. Therefore, this work quantitatively proved the high affinity and specificity of multivalent carbohydrate-protein interactions. Similar affinities were also observed by Liang *et al.* where K_d values in the nM range were obtained [128]. Taking advantage of the high avidity between the lectin and gold glyco-NPs, Lin and coworkers reported the separation of carbohydrate binding proteins from protein mixtures aided by the gold glyco-NPs as affinity probes. Furthermore, using this approach, they determined the identity and the carbohydrate binding epitopes of the proteins by mass spectrometry analysis [112].

Russell, Field and coworkers demonstrated the utility of gold glyco-NPs to detect carbohydrate-binding lectins using colorimetric bioassays [120,129]. Au-NPs have unique surface plasmon absorption. When the particles are close to each other, their plasmon bands can become coupled, resulting in the red shift of absorbance and color change [101]. Upon incubation of gold glyco-NPs with multimeric lectins, the specific bio-recognition between carbohydrate ligands and lectins induced NP aggregation, which was easily observed through the broadening and the red shift of absorbance. Through this assay, the Man-AuNPs yielded a detection limit of 40 nM of Con A. Similar methods have been developed by the Sato group to detect and quantify Con A [130].

During tumor progression, the normal cellular carbohydrate collection is modified resulting in the exposure of "non-self" structures, which are referred to as tumor-associated carbohydrate antigens (TACAs) as exemplified by the Thomsen-Friedenreich (TF) antigen. The disaccharide TF antigen (Gal β 1-3GalNAc) is readily detectable in ~ 90% of all human carcinomas but rarely in normal tissues [131]. Immobilization of TACAs on a polyvalent NP template represents a new strategy to raise strong immune responses *in vivo*. To this end, Barchi and coworkers prepared water-soluble stable Au-NPs coated with the thiol derivatized TF antigen [111]. The TF-AuNP caused aggregation of a TF specific antibody as well as the agglutination of a TF specific lectin, i.e., peanut agglutinin, but not the mannose specific lectin Pisum sativum agglutinin. This validated the functional nature of the TF antigen on the particles. However, the TF-AuNPs prepared were

found to have high polydispersity with non-uniform size distribution, which was presumed to be the cause for inconsistent *in vivo* immunological results [115]. Lowering the TF ligand density afforded more uniform particles, although the immunological evaluations of the new particles have not been reported yet.



5.2.3. Carbohydrate-Cell Interactions

For studying NP-cell interactions, the Penadés groups reported the preparation of gold and gold-iron NPs [132] (average core-size diameters 1.5 - 2.5 nm) functionalized with maltose (Malto), Glc and Lacto and evaluate their biological effects [109]. Different cellular responses were obtained for each glyco-NP type depending on the sugar, demonstrating the importance of carbohydrate in cellular-recognition. With a human fibroblast cell line, Lacto-NPs were shown to be taken up by endocytosis without provoking apoptosis while Malto-NP were endocytosed and promoted cell death (25% of the original cells surviving at NP concentrations higher than 15 μ M). Interestingly, Glc-NPs had a completely different behavior where it was not endocytosed and did not affect cell viability much. Furthermore, different changes in cytoskeleton organization of the cells were observed with the three types of glyco-NPs. Although the exact mechanisms of the differential behavior of the glyco-NPs were not clearly understood, these observations encouraged them to test the possibility of using Glc- or Lacto-NPs to image an experimental C6 glioma in mice *in vivo* which will be discussed later.

Recently, the same group prepared a small library of multivalent Au-NPs functionalized with different structural fragments of the high mannose undecasaccharide of gp120 in various ligand densities and evaluated their effects on the inhibition of HIV glycoprotein gp120 binding to DC-SIGN expressing cells [133]. A major mechanism of HIV infection involved the interaction of gp120 with DC-SIGN expressed on dendritic cells. DC-SIGN recognizes endogenous N-linked high-mannose-type oligosaccharide structures $\text{Man}_9(\text{GlcNAc})_2$ of the HIV envelop glycoprotein gp120 [134]. A highly significant inhibition (~ 20,000-fold more effective in inhibiting DC-SIGN/gp120 interaction) using AuNPs bearing short disaccharide $\text{Man}\alpha 1-2\text{Man}$ (100% inhibition at 115 nM) than those with the corresponding monovalent disaccharide was observed (Fig. 10) [133]. Moreover, inhibition of gp120-DC-SIGN binding was evaluated in a model using DC-SIGN-transfected Raji B cells [135]. Oligomannoside-functionalized AuNPs were able to prevent the HIV DC-SIGN-mediated trans-infection of T cells at nM concentrations, while the AuNPs alone or the non-DC-SIGN binding Glc Au-NPs did not have a significant inhibitory effect on HIV infection. Therefore, they showed a successful carbohydrate-based multivalent system that can function as an anti-adhesive barrier at an early stage of HIV-1 infection, prevent viral attachment to DC-SIGN-expressing cells, and subsequently inhibit trans-infection of human T lymphocytes.

Besides DC-SIGN, gp120 can also interact with cell surface glycolipids such as galactosyl ceramide (GalCer). To inhibit this interaction, Gervay-Hague and coworkers prepared thiol terminated C-glycoside analogs of Gal and Glc and immobilized them onto AuNPs using the *in situ* reduction and coating procedure [113]. Through a competitive assay displacing recombinant gp120 from plate bound GalCer, they demonstrated that the multivalent Gal-

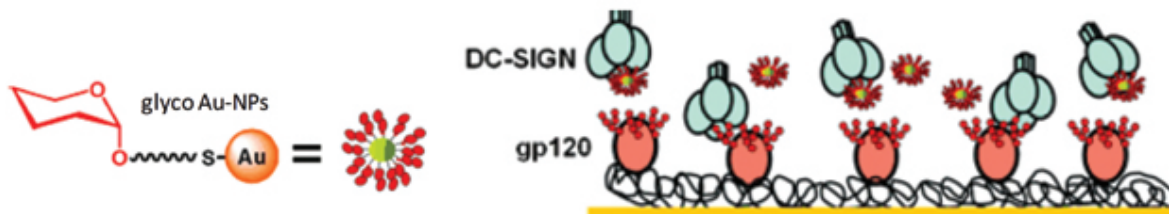


Fig. (10). The glyco Au-NPs can reduce the binding between DC-SIGN and gp120, which have a significant inhibitory effect on HIV infection to cells expressing DC-SIGN [133]. (Copyright Wiley-VCH Verlag GmbH & Co. KGaA. Reproduced with permission).

AuNPs were > 300 times more active than the control carbohydrate disulfides, thus suggesting this nanoplatform can potentially be useful for reducing HIV-1 adhesion to mammalian cells.

5.2.4. Pathogen and Toxin Detection

Pathogens (bacteria, viruses, and other microbes) often use cell-surface carbohydrates to invade host organisms and to deliver toxins. Protein-sugar interactions between the pathogens and the host cells are crucial for the infectious process. Multivalent protein-carbohydrate interactions generate adhesive forces as an effective means of strengthening those binding events. This in turn can enable rapid and sensitive detection of pathogen and toxins using gold glyco-NPs without time-consuming procedures such as incubation or polymerization chain reaction amplification.

At an early stage in this direction, Lin and coworkers demonstrated the specific binding of mannose-encapsulated gold NPs (Man AuNPs) to FimH adhesin in bacterial type 1 pili of *E. coli* by TEM [136]. This was one of the first examples that carbohydrate-functionalized AuNPs could be used as efficient labeling probes and multiligand carriers in a biological system (Fig. 11).

Recently, they designed AuNPs (~ 4 – 20 nm) for Shiga-like toxin detection, separation and inhibition (Fig. 12) [119]. As *E. coli* O157:H7 is a chief cause of foodborne illness, the development of a rapid and sensitive detection method of Shiga toxins (Sts), which are produced by this strain of bacteria, is highly desirable. Sts are a family of AB₅ bacterial toxins, which specifically recognizes cell surface glycosphingolipid globotriaosylceramide (Gb₃) through multivalent binding of the symmetric B-subunit pentamer. The Gb₃ glycolipid is known as the globotriose (P^k) blood group antigen or CD77, which contains the trisaccharide Gal α 1-4Gal β 1-4Glc. Lin and coworkers engineered globotriose-functionalized gold NPs (P^k-AuNP) with variable core sizes and linker length. They demonstrated that a 20 nm water-soluble P^k-AuNP was an antagonist for B-SIt and shows >10⁸-fold binding affinity enhancement over the monovalent P^k trisaccharide using SPR

competition binding assay. Interestingly, linker length had a significant effect on binding affinity with longer linkers resulting in 5 to 75 fold affinity enhancement compared to shorter ones. This was attributed to the greater flexibility of the long linker, rendering it easier for the P^k ligand to bind higher number of sites in the B-SIt pentamer. The core sizes of the NPs also significantly impacted the avidity with larger NPs (20 nm) showing stronger binding than the corresponding smaller NPs (4 nm). This was explained by the smaller surface curvature associated with larger NPs. When the AuNP surface became flatter, the ligands on the AuNP surface could interact with the B-SIt more easily. The high avidity between the GGNPs and Sts enabled the capture of the recombinant Shiga-like toxin I (B-SIt) from bacterial cell lysate with > 95% purity while maintaining its activity [119].

Russell and coworkers developed a simple colorimetric bioassay for the detection and quantification of cholera toxin (CT) within 10 minutes [137]. The bioassay is based on lactose-functionalized AuNPs that upon incubation with the toxin formed aggregates. This resulted in red-shift of the surface plasmon absorption band [101] and a solution color change from red to purple with a limit of detection of 54 nM of CT. The selectivity of the bioassay stems from the thiolated lactose derivative that mimics the GM₁ (Gal(β 1-3)GalNAc[Neu5Ac(α 2-3)]-(β 1-4)Gal(β 1-4)Glc-lipid) ganglioside, the receptor to which cholera toxin binds in the small intestine.

In another example, the Perez group described a NP-based assay to assess bacterial growth by monitoring the plasmon absorbance band of dextran-coated Au-NPs [138]. Upon mixing Con A and dextran coated Au-NPs with the cell culture medium, extensive aggregates were formed resulting in large shifts of the surface plasmon band of the NPs. Under conditions of bacterial growth inhibition, the amounts of free carbohydrates in the medium were high, which competed with the dextran Au-NPs for Con A binding. This would result in blue shift of the maxima of Au-NP absorbance. The differential changes in the surface plasmon bands

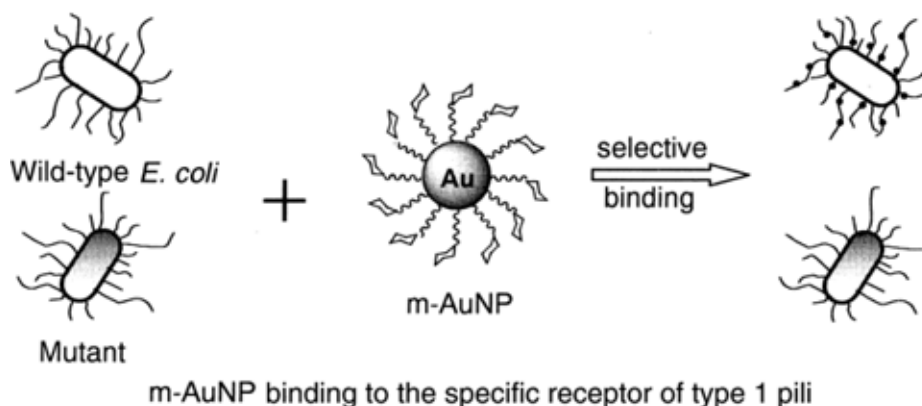


Fig. (11). Selective binding of Man-AuNPs to the wild-type *E. coli* strain ORN178. The mutant ORN208 showed no binding [136]. (Copyright American Chemical Society. Reproduced with permission).

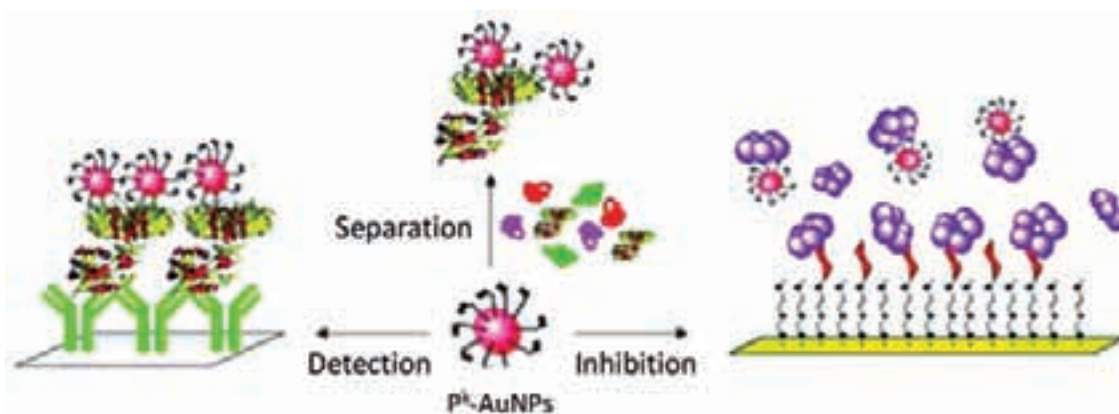


Fig. (12). Schematic presentation of P^k-AuNPs for detection, separation and inhibition of Shiga-like toxin [119]. (Copyright Wiley-VCH Verlag GmbH & Co. KGaA. Reproduced with permission).

of dextran-coated Au-NP upon clustering were used as a quick indicator of the state of growth of bacteria, which was useful for evaluation of anti-microbial compounds.

5.2.5. Gene Transfection

Gold Glyco-NPs have been studied as non-viral gene delivery agents. Au-NPs could be functionalized with cationic glycopolymers or simple monosaccharides such as Glc or Gal together with amine terminated PEG chains [139,140]. These particles were highly efficient DNA-binders, which condensed the plasmids into a compact globular shape. This led to comparable gene transfection efficiencies as the commercially available control Lipofectamine 2000, while bestowing much lower toxicity than Lipofectamine. The active targeting properties of carbohydrates [141,142] were not explored in these studies, which can further enhance the specificity of gene delivery and lower the systemic toxicities.

5.3. In Vivo Applications of Gold Glyco-NPs

Building on the promising *in vitro* results, the *in vivo* applications of Gold Glyco-NPs have been explored both for detection and therapy. With the large surface area of Au-NPs, other moieties such as near IR optical probes and contrast agents can be immobilized onto gold glyco-NPs. Park and coworkers prepared multifunctional gold NPs functionalized for disease detection [143]. The gold NPs (~ 16 nm diameter) were coated with near IR fluorescence (NIRF) dye labeled hyaluronic acid (HA-AuNPs). Due to NP surface energy transfer (NSET) between the dye and AuNPs, the emission of the dye was quenched when it was attached on the surface of the NPs. It is known that reactive oxygen species (ROS) and hyaluronidase (HADase) can cleave HA, which should release the NIRF dye from the AuNP surface resulting in the recovery of emission. Indeed, treatment of HA-AuNPs with ROS (100 μM) or HADase (200 units/ml) led to more than 100 fold increases in NIRF

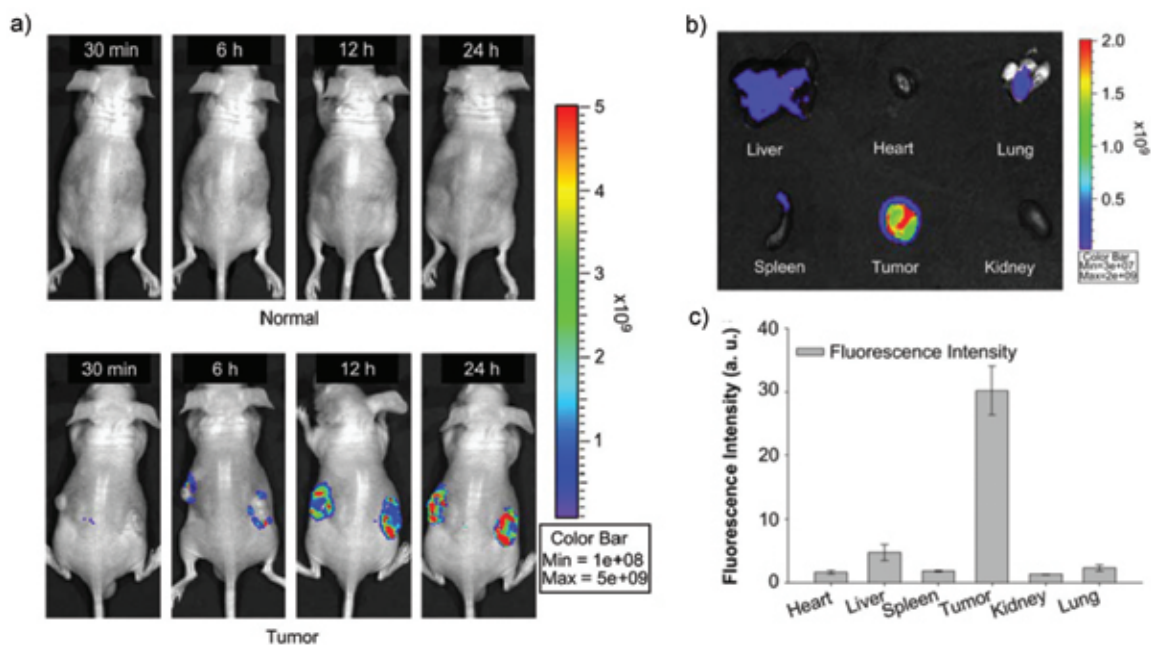


Fig. (13). a) *In vivo* fluorescence images upon intravenous injection of HA-AuNPs (10 pmol) in normal and tumor-bearing nude mice (becoming red color indicates higher NIRF intensity at 671 nm); b) Fluorescence images of 6 different organs obtained from tumor-bearing nude mice after 48 h post-injection of HA-AuNPs. c) Quantification of NIRF intensity in the corresponding organs [143]. (Copyright Elsevier. Reproduced with permission.)

signals. This was corroborated in cellular studies as incubation of HA-AuNPs with activated macrophages and HA-dase secreting cancer cells produced multiple folds of fluorescence intensity enhancement. Furthermore, the authors performed *in vivo* evaluations of these NPs in animal models of rheumatoid arthritis and tumor (Fig. 13). Local inflammation and tumor sites were clearly identified by whole body imaging upon systemic application of the HA-AuNPs. *Ex vivo* examination of the tissues revealed that large amounts of the HA-AuNPs were found to be accumulated in tumor sites (Fig. 13b,c). These results highlight the potential of using glyco-NPs for molecular imaging and disease detections.

The Penadès group developed sugar-coated AuNPs combined with Gd(III) chelates as new paramagnetic probes for MRI [144]. These NPs had small diameters (2–4 nm) and their carbohydrate-coating rendered them non-toxic to cells and mice. It was shown that sugar stereochemistry (Glc, Gal or Lacto) and the relative position of the sugar with respect to the Gd ion affected the relaxivity values of these AuNPs presumably due to the differential interactions with water by the carbohydrate ligands. *In vivo* imaging of glioma in the mouse brain indicated that at the same Gd(III) concentration, Glc-AuNPs gave the best contrast in the tumoral zones compared with Lacto-AuNPs or the commercially available contrast agent, Magnevist.

Besides imaging applications, the Penadès group reported the utilization of Lacto-AuNPs as potent inhibitors of tumor metastasis in mice and evaluated their potential as anti-adhesive tools against metastasis progression [145]. The mouse melanoma B16F10 cells are known to bind with lactose presumably due to the presence of cell surface lectins such as galectins. Pre-incubation of the B16F10 cells with the Lacto-AuNPs prior to injections into mice substantially inhibited the lung metastasis of the tumor (up to 70%), while the corresponding Glc-AuNPs did not have any effects (Fig. 14).

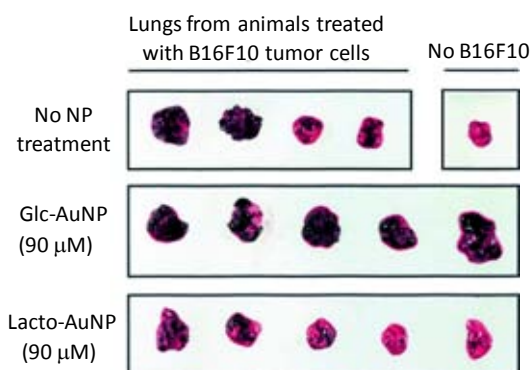


Fig. (14). The incubation of Lacto-AuNPs with mouse melanoma B16F10 cells prior to intravenous inoculation in C57/B16 mice significantly reduced the lung metastasis of the tumor. In comparison, the Glc-AuNPs were ineffective in reducing metastasis [145]. (Copyright Wiley-VCH Verlag GmbH & Co. KGaA. Reproduced with permission).

Mousa and coworkers reported the synthesis of heparin coated AuNPs (HP-AuNPs) [121]. Heparin is a class of naturally occurring polysaccharides, which can inhibit basic fibroblast growth factor-2 induced angiogenesis [146]. The HP-AuNPs were found to have significantly higher anti-angiogenesis efficacy compared with the corresponding Glc-AuNPs. In a mouse model, the HP-AuNPs demonstrated high anti-angiogenesis efficacy without much toxicity, while the free Au was lethal to the animals at the same concentration.

6. GLYCO-QUANTUM DOTS

Quantum dots (QDs) are nanosized fluorescent semiconductors. Compared with organic dyes and fluorescent proteins, QDs have unique optical and electronic properties: i.e., broad absorption spectra, size-tunable emission maximum, high quantum yield, and resistance against photobleaching [38,147]. Coupled with the ability for multivalent display of ligands, these characteristics render carbohydrate immobilized QDs well suited for a variety of biological applications [45,148-156].

6.1. *In Vitro* Applications

QDs protected with polysaccharides were reported in 2003 by the Rosenzweig group [45]. They prepared CdSe-ZnS QDs coated with carboxymethyl dextran and polylysine through electrostatic interactions, and demonstrated that glucose binding protein such as Con A had high affinities with the glyco-QDs. The incubation of the dextran coated QDs with Con A led to the formation of large bright and photostable aggregates allowing lectin detection using a conventional fluorescence microscope. Along the same line, Sun, Chaikof and coworkers reported the site-specific labeling of streptavidin-QDs with glycopolymers terminated with biotin, which retained the specific recognition by lectins [156]. In addition, the Suroliia group coated CdSe-ZnS QDs with thiol terminated carbohydrates and used such glyco-QDs for selective detection of lectins [151]. Barchi and coworkers immobilized the TACA disaccharide antigen TF (gal-β1-3GalNAc) onto QDs [152]. Large clusters of agglutinated TF-QDs were readily observed upon addition of TF-specific monoclonal antibody (mAb) or galactoside binding lectin peanut agglutinin (PNA) but not with the control QD containing no carbohydrates confirming the functional integrity of the antigen on the surface of the QD [152]. Multivalent glyco-QDs could serve as a platform to display carbohydrates for anti-cancer vaccine development.

QDs can be used to detect the presence of lectins on cells. Fang and coworkers prepared CdSe-ZnS QDs in the presence of thiol terminated GlcNAc or Man through an *in situ* reduction and coating procedure and incubated these glyco-NPs with live sperms from mice, pigs and sea-urchin [155]. Interestingly, GlcNAc-encapsulated QDs were found to be concentrated at the sea-urchin sperm heads, while Man-coated QDs tended to spread over the whole body of mouse sperm (Fig. 15). This was presumably due to the different distribution of the GlcNAc and Man receptors on the sperm surface. This work suggested that glyco-QDs can function as useful fluorescent tags for monitoring cellular events. Field, Russell and colleagues also used the *in situ* reduction and coating procedure to fabricate Man coated QDs [157]. They demonstrated that these Man-QDs induced luminescent aggregates of FimH containing *E. coli* strain ORN 178, which led to the detection of *E. coli* with a detection limit of 10^4 cells/mL.

The Aoyama group reported the synthesis of 15 nm QD conjugated with calyx-[4]resorcarene functionalized sugars to study the size-dependence of endocytosis [158]. The usage of QD allowed them to quantify the cellular uptake of the glyco-QDs and monitor their intracellular distribution. It was shown that these QD-conjugated sugar balls were taken up by Hela cells *via* endocytosis. The uptake efficiency was higher than the micellar homoaggregate of the amphiphile (5 nm) but lower than the virus-like conjugate bearing the same carbohydrates (50 nm). Coupled with prior results that aggregates larger than 100 nm were not uptaken effectively, this study suggested 50 nm being the optimal size for endocytosis and it was important to control the size of glyco-nanocomposite for the design of artificial delivery vehicles.

Besides lectin and cellular binding studies, glyco-QDs were used in an innovative approach to detect glycosylation states of proteins. As carbohydrates attached on glycoproteins can play

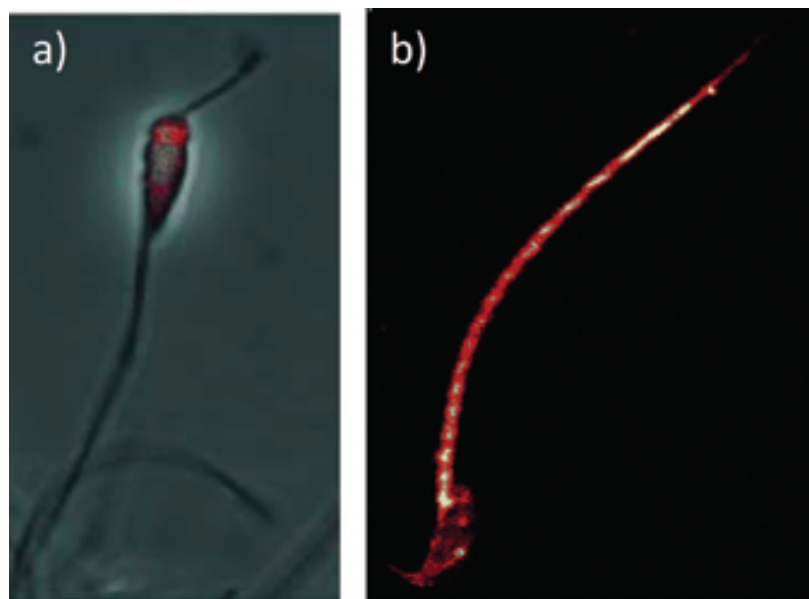


Fig. (15). Confocal microscope images of sperm upon incubation with glycoquantum dots. **a)** GlcNAc-QD labeling was mainly on the heads of sea-urchin sperm (scale bar=20 μ m), and **b)** Man-QD labeled the tail of mouse sperm [155]. (Copyright Wiley-VCH Verlag GmbH & Co. KGaA. Reproduced with permission).

essential roles in determining glycoprotein functions, a simple assay to determine protein glycosylation is desirable. Kim and coworkers prepared dextran coated QDs and Con A immobilized Au-NPs [153]. The binding of Con A with dextran led to quenching of the fluorescence emission of QDs by the Au-NPs due to energy transfer. Addition of glycosylated proteins would compete with dextran-QD for Con A-AuNP binding, resulting in recovery of fluorescence. This allowed rapid and simple detection of degree of protein glycosylation, which was adapted for high throughput analysis of glycoproteins.

6.2. In Vivo Detection

Kim and coworkers reported the fabrication of water-soluble hyaluronic acid-coated QDs (HA-QDs) (~ 50-120 nm depending on mixing ratio QD/HA) where HA was immobilized electrostatically on positively charged QDs [149]. HA-QDs were able to be selectively endocytosed by lymphatic vessel endothelial receptor 1 (LYVE-1) over-expressing lymphatic endothelial cells (LEC) and HeLa cells, but not by LYVE-1 negative human dermal fibroblasts. In contrast, QDs without HA coating were uptaken regardless of cell types. The HA coating reduced the cytotoxicity of the NPs compared with uncoated QDs as determined through cell viability and apoptosis assays. This enabled fluorescence imaging of lymphatic vessels (lymph-angiogenesis) in live mice for more than one day (Fig. 16) [149]. The binding between LYVE-1 and HA-QDs in mice was confirmed by immunohistochemistry, where LYVE-1 and HA-QDs were found to colocalize in mouse tissues.

Besides lymphatic vessel imaging, HA-QDs were used to image liver in cirrhotic mice [159]. Through cellular assays, it was shown that HA-QDs were uptaken more by the cells causing chronic liver diseases such as hepatic stellate cells (HSC-T6) and hepatoma cells (HepG2) than normal hepatocytes (FL83B). Upon administration of HA-QDs to cirrhotic mice, their livers showed greatly enhanced fluorescence. The clearance of the fluorescence from the cirrhotic mouse liver was much slower than that from the normal mice, allowing detection of cirrhotic liver.

Instead of using HA to target liver, the Seeberger group reported the synthesis of carbohydrate (Man, Gal, GalN)-capped

PEGylated QDs (~ 15 - 20 nm) to study *in vivo* liver imaging [148]. They demonstrated that Gal- and GalN-capped QDs were selectively uptaken by hepatocellular carcinoma HepG2 cells *via* the ASGP-R receptor, a galactoside binding asialoglycoprotein expressed predominantly on hepatocytes. The uptake was partially inhibited by pre-incubation with poly-L-lysine galactose polymer or by the knockdown of ASGP-R1 proving that the internalization was *via* receptor-mediated endocytosis. *In vivo*, Man- and GalN-capped QDs accumulated selectively in the liver suggesting the presence of Man and ASGP-R receptors on Kupffer and hepatic cells respectively. It is worth mentioning that the same group recently presented an efficient synthesis of carbohydrate-functionalized QDs in micro flow reactors at 160 $^{\circ}$ C [160].

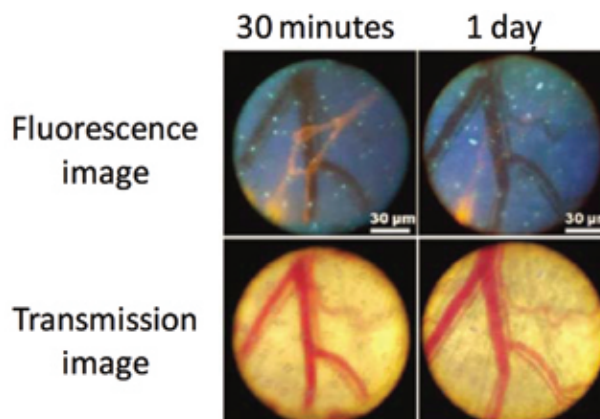


Fig. (16). Upon subcutaneous injection of HA-QDs into mouse ears, fluorescence imaging clearly showed the presence of lymphatic vessels, while they were not visible in transmission images. Images were taken 30 minutes and 1 day after injection [149]. (Copyright American Chemical Society. Reproduced with permission).

7. GLYCO-CARBON NANOTUBES

Carbon nanotubes are allotropes of carbon with a cylindrical nanostructure. Bertozzi and coworkers functionalized single-walled

carbon nanotubes (SWNT) with glycopolymers or glycodendrimers to mimic cell surface proteins [161-163]. Carbohydrates immobilized on the SWNT retained their specific biological recognition as proven by lectin binding. Furthermore, the cytotoxicities of the SWNTs were much reduced with the carbohydrate coating [161].

The Sun group reported that SWNT could serve as an excellent scaffold for multivalent carbohydrate ligand display [164]. The Gal-SWNTs exhibited strong cell adhesion resulting in efficient capturing of pathogenic *E. coli* O157: H7 strain in solution [165]. Moreover, they demonstrated that Man or Gal-functionalized SWNTs bound effectively to *B. anthracis* spores in the presence of a divalent cation [166,167]. This binding resulted in substantial aggregation of the spores and subsequent removal of the spores, which may potentially find applications in the pathogen decontamination and anti-bioterrorism.

8. GLYCO-DENDRIMERS

Dendrimers are a class of “smart” branched monodispersed functional macromolecules with highly ordered symmetrical architecture [168,169]. They consist of a central core, branching units and terminal functional groups. The core dictates the environment of the nanocavities, whereas the external groups determine their solubility and biochemical behavior. When the external groups are modified with saccharides, glyco-dendrimers are produced [170]. Compared with other glyco-nanocomposites, an important feature of glyco-dendrimers is that they have much less polydispersity, which gives better control of surface ligand density and an overall better defined molecular architecture. This is important for quantitative understanding of the binding.

Over the past two decades, many examples of glyco-dendrimers have been reported [170,171]. The major applications of glyco-dendrimers are to enhance the carbohydrate-receptor binding through the multivalent effect. In the following, we will discuss the main biological applications of glyco-dendrimers.

8.1. Probing Carbohydrate-Lectin Binding and Carbohydrate-Carbohydrate Interactions

In an early example of lectin binding, Roy and coworkers prepared mannodendrimers based on the scaffolding of multiantennary branches of L-lysine residues and tested for the inhibition of yeast mannan binding to Con A and pea lectins by enzyme-linked lectin assays [172]. The mannosylated 16-mer dendrimer showed 86 fold increases on per monomer basis in inhibitory potency compared to the corresponding monomeric ligand highlighting the power of multivalency. This phenomenon was corroborated by studies of a variety of other lectins including galectin [173], cholera and shiga toxins [174,175], bacterial toxins [176], PA-IL and PA-IIL lectins from *P. aeruginosa* [177], FimH

from *E. coli*, 178 and a mitogenic lectin from *Pisum sativum* (pea lectin) [179], and the HIV-1 inactivating protein Cyanovirin-N [180].

The Cloninger group prepared G3- through G6-poly(amidoamine) PAMAM dendrimers functionalized with Man, Glc and Gal or mixtures of these carbohydrates in varying ratios, and studied the effects of carbohydrate loading on lectin binding (Fig. 17) [181-184]. They discovered that the amount of sugar on the dendrimer surface had a significant impact on avidity. G(4)- to G(6)-PAMAM dendrimers with 50% Man incorporation showed the highest activity in hemagglutination assays with Con A, while higher Man density actually led to a decrease in lectin binding due to unfavorable steric crowding [183]. Furthermore, they demonstrated that in optimized systems, the binding avidity can be predicted and it is tunable using a mixture of low- and high-affinity ligands.

Instead of studying carbohydrate – protein binding, the Basu group employed the PAMAM dendrimers to examine carbohydrate – carbohydrate interactions. They demonstrated that lactosyl dendrimers engaged in binding with GM3 immobilized in a Langmuir monolayer [185]. This carbohydrate-carbohydrate interaction requires the presence of calcium ion and was dependent on the density of both the carbohydrate on the dendrimer as well as the glycolipid within the monolayer.

8.2. The Interactions between Glyco-Dendrimers and Pathogens

Urinary tract infections (UTIs) are among the most widespread inflammatory diseases caused by uropathogens, predominately *E. coli*, where the bacteria attach to the urinary tract epithelial surface through fimbriae adhesion molecules [186,187]. There are three types of fimbriae: type 1 pili terminated with FimH (Man-specific), long P fimbriae covered with PapG (galabiose (Gal α 1-4Gal)-specific), and flexible F17 fimbriae capped with GafD (GlcNAc-specific) [188]. Oligomannoside-based adhesions are among the most prevalent studied type of carbohydrate-specific bacterial adhesion ligands. *E. coli* adheres to the epithelium using type 1 fimbriae exposing a mannose-binding FimH adhesion at the tip. Inhibition of type 1 pili mediated bacterial attachment using sugar mimetics is thus a promising approach to treat UTIs.

As the FimH crystal structures were available [189,190], structural based ligand design became possible to greatly improve the affinity and specificity of FimH ligands. Various Man-containing oligosaccharides [191] and aromatic α -mannosides [192] that antagonize type 1 fimbriae mediated bacterial adhesion were identified. Aromatic α -mannosides were shown to be 500-1000 times more inhibitory than methyl α -mannoside for the adhesion of type 1 fimbriated *E. coli*. [192]. This is due to the presence of a hydrophobic region next to the monosaccharide-binding site of the fimbriae as recently demonstrated in the X-ray structures [189,190]. It has been shown that α -D-Man based inhibitors of FimH not only

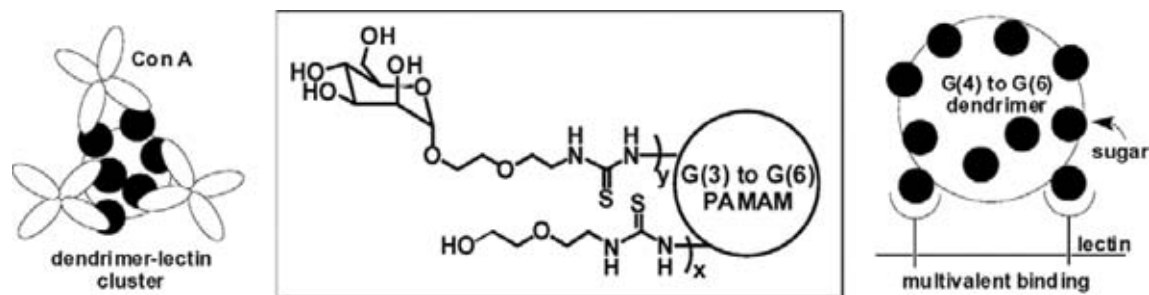
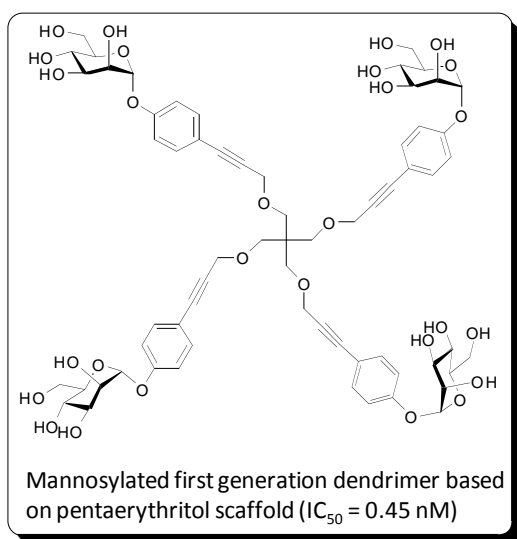


Fig. (17). Schematic cartoon showing the multivalent binding of lectin Con A with G(3) to G(6) PAMAM glycodendrimers [183]. (Copyright American Chemical Society. Reproduced with permission.)

blocked bacterial adhesion on uroepithelial cells but also antagonized invasion. Heptyl-D-mannose prevented the binding of type 1-piliated *E. coli* to the human bladder cell line 5637 and reduced both adhesion and invasion of the UTI89 cystitis isolate instilled in mouse bladder [189].

While monovalent hydrophobic α -D-mannoside binds in the μ M range, a marked increase could be achieved using multivalent presentation of aryl mannoside epitopes. Roy and coworkers reported good inhibitory potencies of a series mannose bearing glyco-dendrimers towards the glycoprotein binding of a type 1 fimbriated *E. coli* K12 strain [193]. The fourth generation of the α linked aromatic mannosyl dendrimer exhibited impressive subnanomolar inhibition ($IC_{50} = 0.9$ nM, 14.4 nM/Man).

Building on this success, the Roy group prepared mannosylated first generation glycodendrimers using pentaerythritol and bis pentaerythritol scaffolds assembled *via* Sonogashira and *click* chemistry [178]. SPR measurements showed that the mannosylated tetramer possessing an aryl moiety in the vicinity of the anomeric oxygen was the best ligand known to date toward *E. coli* K12 FimH with subnanomolar affinities ($K_d = 0.45$ nM, 1.4 nM per Man residue). These clusters were about 5000 times more potent than monovalent Man for their capacity to inhibit the binding of *E. coli* to erythrocytes *in vitro*. This represents potential therapeutic applications for the inhibition of adhesion of *E. coli* toward urothelial infections.



The Pieters group reported the inhibition of live P-fimbriated *E. coli* PapG₉₆ by an octavalent galabiose derivative with an IC_{50} of 2 μ M [194]. PapG₉₆ is the most specific PapG adhesin binding to the terminal galabiose structure. In their studies, it was found that the monovalent ($IC_{50} = 85$ μ M), divalent ($IC_{50} = 30$ μ M), tetravalent ($IC_{50} = 11$ μ M) and PAMAM-8 dendrimer ($IC_{50} = 14$ μ M) were less potent than the octavalent construct ($IC_{50} = 2$ μ M), while free mannose caused no inhibition even at 10 mM concentration.

Besides studying the Gram negative *E. coli*, Pieters and coworkers reported hemagglutination inhibition assays conducted on the Gram-positive bacterium *Streptococcus suis* (*S. suis*) [195]. It was shown that octameric galabioside G(1)-PAMAM dendrimer had a minimal inhibitory concentration ($IC_{50} = 0.3$ nM with a 256-fold improvement over the monovalent galabioside [196]. These results are consistent with the report by Magnusson and coworkers that di- to tetravalent dendritic galabiosides were several hundred times more efficient than the monomeric galabiosides in inhibiting hemagglutination by *S. suis*, resulting in complete abolishment of bacterial adhesion with low nanomolar concentrations of glyco-dendrimers [197]. The anti-adhesive potency could be further

improved by introducing aromatic substituents in the polyvalent construct.

In addition to binding FimH, mannosylated dendrimers can also bind with other biologically significant lectins, such as DC-SIGN. As discussed earlier, DC-SIGN is involved in infection of pathogens such as HIV-1. The Rojo group investigated the inhibition of DC-SIGN mediated Ebola virus infection by mannosyl dendrimers [198,199]. They discovered that a dendrimer bearing 32 mannosyl units was able to directly inhibit DC-SIGN mediated Ebola viral entry into Jurkat cells at nanomolar concentrations ($IC_{50} \sim 337$ nM). In addition, the binding of the glyco-dendrimer with DC-SIGN significantly reduced the binding and transfer of virus to other cells.

8.3. The Interactions between Glyco-Dendrimers and Antibodies/Immunological Cells

Glycodendrimers have been investigated for their interactions with antibodies. To facilitate the development of anti-tumor treatment, Roy, Rittenhouse-Olsen and coworkers prepared glycodendrimers containing the TACA TF disaccharide and studied their interactions with tumor binding mAbs [200]. They found that two tetravalent constructs had IC_{50} values around 18 nM towards inhibiting mAb binding, which represented over 100 folds increase in inhibition over the monomer. Hexavalent dendrimers actually showed lower binding presumably due to unfavorable orientations of the carbohydrate ligands in the hexamer. TF is involved in tumor metastasis to liver by binding tumor cells to the lectin asialoglycoprotein receptor on hepatocytes in the liver. With the strong binding of TACA tetramers, the cancer cell mimetics TACA dendrimers could be used as potential anti-adhesion therapy to block tumor metastasis.

Another interesting application of the glycodendrimers was in anti- α Gal antibody studies [201,202]. α Gal (Gal α 1-3Gal β 1-4GlcNAc) is an antigen expressed on the cells of non-human mammals. Humans have natural anti- α Gal IgM antibodies, which causes hyperacute rejection of pig organs thus hampering primate xenotransplantation. Thus, removing anti- α Gal antibodies represents a novel avenue to facilitate xenotransplantation. The Thoma group synthesized glycodendrimers containing the α Gal trisaccharide epitopes, which spontaneously self assembled in water to form NPs. The third generation α Gal dendrimer showed an impressive nM inhibition of anti- α Gal IgM and α Gal mediated lysis of pig erythrocytes. Furthermore, *in vivo* evaluation in monkeys showed that anti- α Gal IgM concentration was significantly reduced upon administration of the α Gal dendrimer and anti- α Gal IgM mediated haemolytic activity was completely eliminated.

Shaunak and coworkers prepared two types of PAMAM glycodendrimers, one bearing glucosamine (GlcN) and the other glucosamine 6-sulfate (6-O GlcN) [203]. They discovered that the GlcN dendrimers was capable of inhibiting lipopolysaccharide mediated activation of dendritic cells and macrophages, while neither the dendrimers core or monomeric GlcN had any effect. This is probably due to receptor crosslinking by the dendritic GlcN structures. In addition, the 6-O GlcN glycodendrimers blocked endothelial cell proliferation and angiogenesis. Administration of these two glyco-dendrimers together in a rabbit model led to an impressive reduction of scar tissue formation following glaucoma filtration surgery, which was critical for the long term success of the surgery.

Bezouška, Krěn and coworkers investigated the effects of glycodendrimers on natural killer cells, an important class of immunological cells with major roles in rejection of tumors and virally infected cells. Aminosugars such as GlcNAc and N-acetyl mannosamine are known to have a high affinity for the natural killer cell protein-1A (NKR-P1A) protein, the major activating

receptor on the surface of natural killer cells. GlcNAc-containing glycodendrimers displayed strong *in vitro* affinity ($IC_{50} \sim 10^{-9}$ M) for NK-R-PIA [204-206]. Administration of these compounds *in vivo* resulted in a substantial increase in the antitumor activity with the activation of the natural killer cells [207]. Furthermore, the glycodendrimers induced up-regulation of antibody formation due to NK cell stimulation [208].

9. CONCLUSIONS AND FUTURE OUTLOOK

In this review, we have discussed the applications of a variety of glyco-nanocomposites including magnetic NPs, gold NPs, quantum dots, carbon nanotubes and dendrimers. It is clear that the avidity between carbohydrates and receptors can be greatly enhanced through multivalent display of carbohydrates on nanomaterials. By combining the multi-faceted biological functions of carbohydrates with unique properties of nanomaterials, significant advancements have been achieved during the past decade in this field. This includes better understanding of carbohydrate-carbohydrate, carbohydrate-protein interactions, better and faster method for pathogen detection and decontamination, tumor inhibition, as well as promising *in vivo* molecular and cellular imaging applications. To fully realize the potential of glyco-nanotechnology especially for future clinical applications, better fundamental knowledge of how NPs interact with biological systems is required. Parameters such as size, shape, surface charge, ligand type, and ligand density should be optimized to achieve desired biological functions. Furthermore, bio-distribution, clearance and long term side effect/toxicity of glyco-nanocomposites need to be established. With the importance of carbohydrates in human physiology and pathology firmly established, there are great potential for functionalized glyco-nanoprobes to play significant roles in biomedical applications for many years to come. A taste of sugar has already been around us, but we have just started to explore. As Dr. Richard Feynman famously proclaimed 50 years ago, "there's plenty of room at the bottom".

ACKNOWLEDGEMENT

We are grateful for a CAREER award from the National Science Foundation (CHE0852308) and a predoctoral fellowship from the American Heart Association for financial support.

REFERENCES

- Pankhurst, Q. A.; Thanh, N. K. T.; Jones, S. K.; Dobson, J. Progress in Applications of Magnetic Nanoparticles in Biomedicine; *J. Phys. D: Appl. Phys.* **2009**, *42*, 224001
- Huang, X.; Neretina, S.; El-Sayed, M. A. Gold Nanorods: from Synthesis and Properties to Biological and Biomedical Applications; *Adv. Mater.* **2009**, *21*, 4880-4910 and references therein.
- Peer, D.; Karp, J. M.; Hong, S.; Farokhzad, O. C.; Margalit, R.; Langer, R. Nanocarriers as an Emerging Platform for Cancer Therapy; *Nat. Nanotech.* **2007**, *2*, 751-760.
- Ferrari, M. Cancer Nanotechnology: Opportunities and Challenges; *Nature Rev. Cancer* **2005**, *5*, 161-171.
- Gabius, H.-J.; Siebert, H.-C.; André, S.; Jiménez-Barbero, J.; Rüdiger, H. Chemical Biology of the Sugar Code; *ChemBioChem* **2004**, *5*, 740-764.
- Hakomori, S. Glycosylation Defining Cancer Malignancy: New Wine in an Old Bottle; *Proc. Natl. Acad. Sci., USA* **2002**, *99*, 10231-10233.
- Dwek, R. A. Glycobiology: Toward Understanding the Function of Sugars; *Chem. Rev.* **1996**, *96*, 683-720.
- For other reviews on this subject, see refs 8-10. García, I.; Marradi, M.; Penadés, S. Glyconanoparticles: Multifunctional Nanomaterials for Biomedical Applications; *Nanomedicine* **2010**, *5*, 777-792.
- de la Fuente, J. M.; Penadés, S. Glyconanoparticles: Types, Synthesis and Applications in Glycoscience, Biomedicine and Material Science; *Biochim. Biophys. Acta.* **2006**, *1760*, 636-651 and references cited therein.
- Larsen, K.; Thygesen, M. B.; Guillaumie, F.; Willats, W. G. T.; Jensen, K. J. Solid-phase Chemical Tools for Glycobiology; *Carbohydr. Res.* **2006**, *341*, 1209-1234.
- Gabius, H.-J. Glycans: Bioactive Signals Decoded by Lectins; *Biochem. Soc. Trans.* **2008**, *36*, 1491-1496.
- Varki, A. Biological Roles of Oligosaccharides: All of the Theories are Correct; *Glycobiology* **1993**, *3*, 97-130.
- Seeberger, P. H.; Werz, D. B. Synthesis and Medical Applications of Oligosaccharides; *Nature* **2007**, *446*, 1046-1051.
- Raman, R.; Sasisekharan, V.; Sasisekharan, R. Structural Insights into Biological Roles of Protein-Glycosaminoglycan Interactions; *Chem. Biol.* **2005**, *12*, 267-277.
- Werz, D. B.; Seeberger, P. H. Carbohydrates as the Next Frontier in Pharmaceutical Research; *Chem. Eur. J.* **2005**, *11*, 3194-3206.
- Koeller, K. M.; Wong, C.-H. Emerging Themes in Medicinal Glycoscience; *Nature Biotech.* **2000**, *18*, 835-841.
- Rabinovich, G. A.; Toscano, M. A. Turning 'Sweet' on Immunity: Galectin-glycan Interactions in Immune Tolerance and Inflammation; *Nature Rev. Cancer* **2009**, *9*, 338-352.
- Macher, B. A.; Galili, U. The Gal α 1,3Gal β 1,4GlcNAc-R (α -Gal) Epitope: A Carbohydrate of Unique Evolution and Clinical Relevance; *Biochim. Biophys. Acta* **2008**, *1780*, 75-88.
- Simanek, E. E.; McGarvey, G. J.; Jablonowski, J. A.; Wong, C.-H. Selectin-Carbohydrate Interactions: From Natural Ligands to Designed Mimics; *Chem. Rev.* **1998**, *98*, 833-862.
- Nangia-Makker, P.; Conklin, J.; Hogan, V.; Raz, A. Carbohydrate-binding Proteins in Cancer, and Their Ligands as Therapeutic Agents; *Trends Mol. Med.* **2002**, *8*, 187-192.
- Hakomori, S.-I.; Zhang, Y. Glycosphingolipid Antigens and Cancer Therapy; *Chem. Biol.* **1997**, *4*, 97-104.
- Pieters, R. J. Maximising Multivalency Effects in Protein-carbohydrate Interactions; *Org. Biomol. Chem.* **2009**, *7*, 2013-2025.
- Lingwood, C. A. Oligosaccharide Receptors for Bacteria: a View to a Kill; *Curr. Opin. Chem. Biol.* **1998**, *2*, 695-700.
- Petitou, M.; van Beoekel, C. A. A. A Synthetic Antithrombin III Binding Pentasaccharide Is Now a Drug! What Comes Next?; *Angew. Chem. Int. Ed.* **2004**, *43*, 3118-3133.
- Mammen, M.; Choi, S. K.; Whitesides, G. M. Polyvalent Interactions in Biological Systems: Implications for Design and Use of Multivalent Ligands and Inhibitors; *Angew. Chem. Int. Ed.* **1998**, *37*, 2754-2794.
- Lee, Y. C.; Lee, R. T. Carbohydrate-Protein Interactions: Basis of Glycobiology; *Acc. Chem. Res.* **1995**, *28*, 321-7.
- Lundquist, J. J.; Toone, E. J. The Cluster Glycoside Effect; *Chem. Rev.* **2002**, *102*, 555-578.
- Iqbal, S. S.; Mayo, M. W.; Bruno, J. G.; Bronk, B. V.; Batt, C. A.; Chambers, J. P. A Review of Molecular Recognition Technologies for Detection of Biological Threat Agents; *Biosens. Bioelectron.* **2000**, *15*, 549-578.
- Wang, Z.; Huang, X. Strategies in Oligosaccharide Synthesis; In *Comprehensive Glycoscience from Chemistry to Systems Biology* Kamerling, J. P., Ed.; Elsevier: **2007**; Vol. 1, p 379-413.
- Laurent, S.; Forge, D.; Port, M.; Roch, A.; Robic, C.; Vander Elst, L.; Muller, R. N. Magnetic Iron Oxide Nanoparticles: Synthesis, Stabilization, Vectorization, Physicochemical Characterizations, and Biological Applications; *Chem. Rev.* **2008**, *108*, 2064-2110.
- Jun, Y.-W.; Lee, J.-H.; Cheon, J. Chemical Design of Nanoparticle Probes for High-performance Magnetic Resonance Imaging; *Angew. Chem., Int. Ed.* **2008**, *47*, 5122-5135.
- Lu, A. H.; Salabas, E. L.; Schueth, F. Magnetic Nanoparticles: Synthesis, Protection, Functionalization, and Application; *Angew. Chem., Int. Ed.* **2007**, *46*, 1222-1244.
- Cheng, F. Y.; Su, C. H.; Yang, Y. S.; Yeh, C. S.; Tsai, C. Y.; Wu, C. L.; Wu, M. T.; Shieh, D. B. Characterization of Aqueous Dispersions of Fe $_3$ O $_4$ Nanoparticles and Their Biomedical Applications; *Biomaterials* **2005**, *26*, 729-738.
- Isaac, K.; Wang, X.; Varughese, B.; Isaacs, L.; Ehrman, S. H.; English, D. S. Magnetic Iron Oxide Nanoparticles for Biorecognition: Evaluation of Surface Coverage and Activity; *J. Phys. Chem. B* **2006**, *110*, 1553-1558.
- Gupta, A. K.; Gupta, M. Synthesis and Surface Engineering of Iron Oxide Nanoparticles for Biomedical Applications; *Biomaterials* **2005**, *26*, 3995-4021.
- Jain, P. K.; Huang, X.; El-Sayed, I. H.; El-Sayed, M. A. Noble Metals on the Nanoscale: Optical and Photothermal Properties and Some Applications in Imaging, Sensing, Biology, and Medicine; *Acc. Chem. Res.* **2008**, *41*, 1578-1586.
- Qian, X.; Peng, X.-H.; Ansari, D. O.; Yin-Goen, Q.; Chen, G. Z.; Shin, D. M.; Yang, L.; Young, A. N.; Wang, M. D.; Nie, S. *In vivo* Tumor Targeting and Spectroscopic Detection with Surface-enhanced Raman Nanoparticle Tags; *Nat. Biotechnol.* **2008**, *26*, 83-90.
- Gao, X.; Cui, Y.; Levenson, R. M.; Chung, L. W. K.; Nie, S. *In vivo* Cancer Targeting and Imaging with Semiconductor Quantum Dots; *Nature Biotechnol.* **2004**, *22*, 969-976.
- Qiao, R.; Yang, C.; Gao, M. Superparamagnetic Iron Oxide Nanoparticles: from Preparations to *in vivo* MRI Applications; *J. Mater. Chem.* **2009**, *19*, 6274-6293.
- Lee, J.-H.; Huh, Y.-M.; Jun, Y.-w.; Seo, J.-w.; Jang, J.-t.; Song, H.-T.; Kim, S.; Cho, E.-J.; Yoon, H.-G.; Suh, J.-S.; Cheon, J. Artificially Engineered Magnetic Particles for Ultra-sensitive Molecular Imaging; *Nat. Med.* **2007**, *13*, 95-99.

- [41] Yang, L.; Peng, X.-H.; Wang, Y. A.; Wang, X.; Cao, Z.; Ni, C.; Karna, P.; Zhang, X.; Wood, W. C.; Gao, X.; Nie, S.; Mao, H. Receptor-Targeted Nanoparticles for *In vivo* Imaging of Breast Cancer; *Clin. Cancer Res.* **2009**, *15*, 4722-4732.
- [42] Stoeva, S. I.; Lee, J.-S.; Smith, J. E.; Rosen, S. T.; Mirkin, C. A. Multiplexed Detection of Protein Cancer Markers with Biobarcode Nanoparticle Probes; *J. Am. Chem. Soc.* **2006**, *128*, 8378-8379.
- [43] van Kasteren, S. I.; Campbell, S. J.; Serres, S.; Anthony, D. C.; Sibson, N. R.; Davis, B. G. Glyconanoparticles Allow Pre-symptomatic *in vivo* Imaging of Brain Disease; *Proc. Natl. Acad. Sci., USA* **2009**, *106*, 18-23.
- [44] Paul, K. G.; Frigo, T. B.; Groman, J. Y.; Groman, E. V. Synthesis of Ultrasmall Superparamagnetic Iron Oxides Using Reduced Polysaccharides; *Bioconjugate Chem.* **2004**, *15*, 394-401.
- [45] Chen, Y.; Ji, T.; Rosenzweig, Z. Synthesis of Glyconanospheres Containing Luminescent CdSe-ZnS Quantum Dots; *Nano Lett.* **2003**, *3*, 581-584.
- [46] Hu, Y.; Jiang, X.; Ding, Y.; Ge, H.; Yuan, Y.; Yang, C. Synthesis and Characterization of Chitosan-poly(acrylic acid) Nanoparticles; *Biomaterials* **2002**, *23*, 3193-3201.
- [47] Moore, A.; Marecos, E.; Bogdanov, A., Jr.; Weissleder, R. Tumoral Distribution of Long-circulating Dextran-coated Iron Oxide Nanoparticles in a Rodent Model; *Radiology* **2000**, *214*, 568-574.
- [48] Wang, Y. X.; Hussain, S. M.; Krestin, G. P. Superparamagnetic Iron Oxide Contrast Agents: Physicochemical Characteristics and Applications in MR Imaging; *Eur. Radiol.* **2001**, *11*, 2319-31.
- [49] Lin, P.-C.; Tseng, M.-C.; Su, A.-K.; Chen, Y.-J.; Lin, C.-C. Functionalized Magnetic Nanoparticles for Small-Molecule Isolation, Identification, and Quantification; *Anal. Chem.* **2007**, *3401*-3408.
- [50] Perez, J. M.; Josephson, L.; O'Loughlin, T.; Hogemann, D.; Weissleder, R. Magnetic Relaxation Switches Capable of Sensing Molecular Interactions; *Nat. Biotechnol.* **2002**, *20*, 816-20.
- [51] Perez, J. M.; Josephson, L.; Weissleder, R. Use of Magnetic Nanoparticles as Sensors to Probe for Molecular Interactions; *ChemBioChem* **2004**, *5*, 261-264.
- [52] Jun, Y. W.; Huh, Y. M.; Choi, J. S.; Lee, J. H.; Song, H. T.; Kim, S.; Yoon, S.; Kim, K. S.; Shin, J. S.; Suh, J. S.; Cheon, J. Nanoscale Size Effect of Magnetic Nanocrystals and Their Utilization for Cancer Diagnosis via Magnetic Resonance Imaging; *J. Am. Chem. Soc.* **2005**, *127*, 5732-5733.
- [53] Yu, M. K.; Jeong, Y. Y.; Park, J.; Park, S.; Kim, J. W.; Min, J. J.; Kim, K.; Jon, S. Drug-loaded Superparamagnetic Iron Oxide Nanoparticles for Combined Cancer Imaging and Therapy *in vivo*; *Angew. Chem., Int. Ed.* **2008**, *47*, 5362-5365.
- [54] Park, J.-H.; von Maltzahn, G.; Zhang, L.; Schwartz, M. P.; Ruoslahti, E.; Bhatia, S. N.; Sailor, M. J. Magnetic Iron Oxide Nanoworms for Tumor Targeting and Imaging; *Adv. Mater.* **2008**, *20*, 1630-1635.
- [55] Gao, B. J.; Li, L.; Ho, P. L.; Mak, G. C.; Gu, H.; Xu, B. Combining Fluorescent Probes and Biofunctional Magnetic Nanoparticles for Rapid Detection of Bacteria in Human Blood; *Adv. Mater.* **2006**, *18*, 3145-3148.
- [56] Shukoor, M. I.; Natalio, F.; Tahir, M. N.; Ksenofontov, V.; Therese, H. A.; Theato, P.; Schroeder, H. C.; Mueller, W. E. G.; Tremel, W. Superparamagnetic g-Fe₃O₃ Nanoparticles with Tailored Functionality for Protein Separation; *Chem. Commun.* **2007**, 4677-4679.
- [57] Massart, R. Preparation of aqueous magnetic liquids in alkaline and acidic media; *IEEE Trans. Magn.* **1981**, *17*, 1247-8.
- [58] Koh, I.; Wang, X.; Varughese, B.; Isaacs, L.; Ehrman, S. H.; English, D. S. Magnetic Iron Oxide Nanoparticles for Biorecognition: Evaluation of Surface Coverage and Activity; *J. Phys. Chem. B* **2006**, *110*, 1553-1558.
- [59] Bruce, I. J.; Sen, T. Surface Modification of Magnetic Nanoparticles with Alkoxysilanes and Their Application in Magnetic Bioseparations; *Langmuir* **2005**, *21*, 7029-7035.
- [60] Yamaura, M.; Camilo, R. L.; Sampaio, L. C.; Macedo, M. A.; Nakamura, M.; Toma, H. E. Preparation and Characterization of (3-Aminopropyl)triethoxysilane-coated Magnetite Nanoparticles; *J. Magn. Mater.* **2004**, *279*, 210-217.
- [61] Klotz, M.; Ayral, A.; Guizard, C.; Menager, C.; Cabuil, V. Silica Coating on Colloidal Maghemite Particles; *J. Colloid Interface Sci.* **1999**, *220*, 357-361.
- [62] Corot, C.; Robert, P.; Idee, J.-M.; Port, M. Recent Advances in Iron Oxide Nanocrystal Technology for Medical Imaging; *Adv. Drug Delivery Rev.* **2006**, *58*, 1471-1504.
- [63] Sun, S.; Zeng, H. Size-Controlled Synthesis of Magnetite Nanoparticles; *J. Am. Chem. Soc.* **2002**, *124*, 8204-8205.
- [64] Sun, S.; Zeng, H.; Robinson, D. B.; Raoux, S.; Rice, P. M.; Wang, S. X.; Li, G. Monodisperse MFe₂O₄ (M = Fe, Co, Mn) Nanoparticles; *J. Am. Chem. Soc.* **2004**, *126*, 273-279.
- [65] Hyeon, T.; Lee, S. S.; Park, J.; Chung, Y.; Na, H. B. Synthesis of Highly Crystalline and Monodisperse Maghemite Nanocrystallites without a Size-Selection Process; *J. Am. Chem. Soc.* **2001**, *123*, 12798-12801.
- [66] Park, J.; An, K.; Hwang, Y.; Park, J.-G.; Noh, H.-J.; Kim, J.-Y.; Park, J.-H.; Hwang, N.-M.; Hyeon, T. Ultra-large-scale Syntheses of Monodisperse Nanocrystals; *Nature Mater.* **2004**, *3*, 891-895.
- [67] De Palma, R.; Peeters, S.; Van Bael, M. J.; Van den Rul, H.; Bonroy, K.; Laureyn, W.; Mullens, J.; Borghs, G.; Maes, G. Silane Ligand Exchange to Make Hydrophobic Superparamagnetic Nanoparticles Water-dispersible; *Chem. Mater.* **2007**, *19*, 1821-1831.
- [68] Horák, D.; Babič, M.; Jendelová, P.; Herynek, V.; Trchová, M.; Pientka, Z.; Pollert, E.; Hájek, M.; Syková, E. D-Mannose-Modified Iron Oxide Nanoparticles for Stem Cell Labeling; *Bioconjugate Chem.* **2007**, *18*, 635-644.
- [69] Palmacci, S.; Josephson, L.; Groman, E. V. Synthesis of polymer-covered superparamagnetic oxide colloids for magnetic resonance contrast agents or other applications; (Advanced Magnetics, Inc., USA). **1995**; US Patent WO/1995/005669, p 45 pp.
- [70] Shi, Z.; Neoh, K. G.; Kang, E. T.; Shuter, B.; Wang, S.-C.; Poh, C.; Wang, W. (Carboxymethyl)chitosan-Modified Superparamagnetic Iron Oxide Nanoparticles for Magnetic Resonance Imaging of Stem Cells; *ACS Appl. Mater. Interface.* **2009**, *1*, 328-335.
- [71] Srinivasan, B.; Huang, X. Functionalization of magnetic nanoparticles with organic molecules: loading level determination and evaluation of linker length effect on immobilization; *Chirality* **2008**, *20*, 265-277.
- [72] El-Boubbou, K.; Zhu, D. C.; Vasileiou, C.; Borhan, B.; Prospero, D.; Li, W.; Huang, X. Magnetic Glyco-nanoparticles: a Tool to Detect, Differentiate, and Unlock the Glyco-codes of Cancer via Magnetic Resonance Imaging; *J. Am. Chem. Soc.* **2010**, *132*, 4490-4499.
- [73] El-Boubbou, K.; Gruden, C.; Huang, X. Magnetic Glyco-nanoparticles: A Unique Tool for Rapid Pathogen Detection, Decontamination, and Strain Differentiation; *J. Am. Chem. Soc.* **2007**, *129*, 13392-13393.
- [74] Lin, P.-C.; Ueng, S.-H.; Yu, S.-C.; Jan, M.-D.; Adak, A. K.; Yu, C.-C.; Lin, C.-C. Surface Modification of Magnetic Nanoparticle via Cu(I)-Catalyzed Alkyne-azide [2 + 3] Cycloaddition; *Org. Lett.* **2007**, *9*, 2131-2134.
- [75] Pera, N. P.; Kouki, A.; Haataja, S.; Branderhorst, H. M.; Liskamp, R. M. J.; Visser, G. M.; Finne, J.; Pieters, R. J. Detection of Pathogenic Streptococcus suis Bacteria using Magnetic Glycoparticles; *Org. Biomol. Chem.* **2010**, *8*, 2425-2429.
- [76] Hatch, D. M.; Weiss, A. A.; Kale, R. R.; Iyer, S. S. Biotinylated Bi- and Tetra-antennary Glycoconjugates for Escherichia coli Detection; *ChemBioChem* **2008**, *9*, 2433-2442.
- [77] Liu, L.-H.; Dietsch, H.; Schurtenberger, P.; Yan, M. Photoinitiated Coupling of Unmodified Monosaccharides to Iron Oxide Nanoparticles for Sensing Proteins and Bacteria; *Bioconjugate Chem.* **2009**, *20*, 1349-1355.
- [78] Shimura, K.; Kasai, K. Determination of the Affinity Constants of Concanavalin A for Monosaccharides by Fluorescence Affinity Probe Capillary Electrophoresis; *Anal. Biochem.* **1995**, *227*, 186-194.
- [79] Finlay, B. B.; Cossart, P. Exploitation of Mammalian Host Cell Functions by Bacterial Pathogens; *Science* **1997**, *276*, 718-725.
- [80] Beachey, E. H. Bacterial Adherence: Adhesin-receptor Interactions Mediating the Attachment of Bacteria to Mucosal Surfaces; *J. Infect. Dis.* **1981**, *143*, 325-45.
- [81] Levy, S. B. Antibiotic Resistance - the Problem Intensifies; *Adv. Drug Delivery Rev.* **2005**, *57*, 1446-1450.
- [82] Harris, S. L.; Spears, P. A.; Havell, E. A.; Hamrick, T. S.; Horton, J. R.; Orndorff, P. E. Characterization of *Escherichia coli* Type 1 Pilus Mutants with Altered Binding Specificities; *J. Bacteriol.* **2001**, *183*, 4099-4102.
- [83] Lee, Y.; Lee, H.; Kim, Y. B.; Kim, J.; Hyeon, T.; Park, H.; Messersmith, P. B.; Park, T. G. Bioinspired Surface Immobilization of Hyaluronic Acid on Monodisperse Magnetite Nanocrystals for Targeted Cancer Imaging; *Adv. Mater.* **2008**, *20*, 4154-4157.
- [84] Sy, M.-S.; Mori, H.; Liu, D. CD44 as a Marker in Human Cancers; *Curr. Opin. Oncol.* **1997**, *9*, 108-112.
- [85] Kumar, A.; Sahoo, B.; Montpetit, A.; Behera, S.; Lockey, R. F.; Mohapatra, S. S. Development of Hyaluronic Acid-Fe₃O₃ Hybrid Magnetic Nanoparticles for Targeted Delivery of Peptides; *Nanomedicine* **2007**, *3*, 132-137.
- [86] Kamat, M.; El-boubbou, K.; Zhu, D. C.; Lansdell, T.; Lu, X.; Li, W.; Huang, X. Hyaluronic Acid Immobilized Magnetic Nanoparticles for Active Targeting and Imaging of Macrophages; *Bioconjugate Chem.* **2010**, *21*, 2128-2135.
- [87] Wright, A. T.; Anslin, E. V. Differential Receptor Arrays and Assays for Solution-based Molecular Recognition; *Chem. Soc. Rev.* **2006**, *35*, 14-28.
- [88] Lu, C.-W.; Hung, Y.; Hsiao, J.-K.; Yao, M.; Chung, T.-H.; Lin, Y.-S.; Wu, S.-H.; Hsu, S.-C.; Liu, H.-M.; Mou, C.-Y.; Yang, C.-S.; Huang, D.-M.; Chen, Y.-C. Bifunctional Magnetic Silica Nanoparticles for Highly Efficient Human Stem Cell Labeling; *Nano Lett.* **2007**, *7*, 149-154.
- [89] Song, H.-T.; Choi, J.-s.; Huh, Y.-M.; Kim, S.; Jun, Y.-w.; Suh, J.-S.; Cheon, J. Surface Modulation of Magnetic Nanocrystals in the Development of Highly Efficient Magnetic Resonance Probes for Intracellular Labeling; *J. Am. Chem. Soc.* **2005**, *127*, 9992-9993.
- [90] Babi, M.; Horák, D.; Trchová, M.; Jendelová, P.; Glogarová, K.; Lesný, P.; Herynek, V.; Hájek, M.; Syková, E. Poly(l-lysine)-Modified Iron Oxide Nanoparticles for Stem Cell Labeling; *Bioconjugate Chem.* **2008**, *19*, 740-750.
- [91] Park, B. H. J.; Lee, G. H.; Kim, T. J.; Lee, Y. J.; Kim, J. Y.; Kim, Y. W. J.; Chang, Y. M. Comparison of Labeling Efficiency of Different Magnetic Nanoparticles into Stem Cell; *Colloids Surf., A* **2008**, *313*-314, 145-149.
- [92] Yoo, M. K.; Kim, I. Y.; Kim, E. M.; Jeong, H.-J.; Lee, C.-M.; Jeong, Y. Y.; Akaike, T.; Cho, C. S. Superparamagnetic Iron Oxide Nanoparticles Coated with Galactose-carrying Polymer for Hepatocyte Targeting; *J. Biomed. Biotechnol.* **2007**, 94740.
- [93] Lee, R. T.; Myers, R. W.; Lee, Y. C. Further Studies on the Binding Characteristics of Rabbit Liver Galactosyl N-Acetylgalactosamine-Specific Lectin; *Biochemistry* **1982**, *21*, 6292-6298.

- [94] Yoo, M. K.; Park, I. Y.; Kim, I. Y.; Park, I. K.; Kwon, J.-S.; Jeong, H.-J.; Jeong, Y. Y.; Cho, S. C. Superparamagnetic Iron Oxide Nanoparticles Coated with Mannan for Macrophage Targeting; *J. Nanosci. Nanotechnol.* **2008**, *8*, 5196-5202.
- [95] Barthel, S. R.; Gavino, J. D.; Descheny, L.; Dimitroff, C. J. Targeting Selectins and Selectin Ligands in Inflammation and Cancer; *Exp. Opin. Ther. Targets* **2007**, *11*, 1473-1491.
- [96] Eustis, S.; El-Sayed, M. A. Why Gold Nanoparticles are More Precious than Pretty Gold: Noble Metal Surface Plasmon Resonance and its Enhancement of the Radiative and Nonradiative Properties of Nanocrystals of Different Shapes; *Chem. Soc. Rev.* **2006**, *35*, 209-217.
- [97] Nikoobakht, B.; El-Sayed, M. A. Surface-Enhanced Raman Scattering Studies on Aggregated Gold Nanorods; *J. Phys. Chem. A* **2003**, *107*, 3372-3378.
- [98] Huang, X.; El-Sayed, I. H.; Qian, W.; El-Sayed, M. A. Cancer Cell Imaging and Photothermal Therapy in the Near-Infrared Region by Using Gold Nanorods; *J. Am. Chem. Soc.* **2006**, *128*, 2115-2120.
- [99] Thompson, D. Michael Faraday's Recognition of Ruby Gold: the Birth of Modern Nanotechnology; *Gold Bull.* **2007**, *40*, 267-269.
- [100] Grzelczak, M.; Pérez-Juste, J.; Mulvaney, P.; Liz-Marzán, L. M. Shape Control in Gold Nanoparticle Synthesis; *Chem. Soc. Rev.* **2008**, *37*, 1783 - 1791.
- [101] Ghosh, S. K.; Pal, T. Interparticle Coupling Effect on the Surface Plasmon Resonance of Gold Nanoparticles: From Theory to Applications; *Chem. Rev.* **2007**, *107*, 4797-4862.
- [102] Daniel, M.-C.; Astruc, D. Gold Nanoparticles: Assembly, Supramolecular Chemistry, Quantum-Size-Related Properties, and Applications toward Biology, Catalysis, and Nanotechnology; *Chem. Rev.* **2004**, *104*, 293-346.
- [103] Frens, G. Controlled Nucleation for the Regulation of the Particle Size in Monodisperse Gold Suspensions; *Nature* **1973**, *241*, 20-2.
- [104] Turkevich, J.; Stevenson, P. C.; Hillier, J. The Nucleation and Growth Processes in the Synthesis of Colloidal Gold; *Discuss. Faraday Soc.* **1951**, *11*, 55-75.
- [105] Turkevich, J.; Hubbell, H. H. Low-angle x-ray Diffraction of Colloidal Gold and Carbon Black; *J. Am. Chem. Soc.* **1951**, *73*, 1-7.
- [106] Brust, M.; Walker, M.; Bethell, D.; Schiffrin, D. J.; Whyman, R. Synthesis of Thiol-derivatized Gold Nanoparticles in a Two-phase Liquid-liquid System; *Chem. Commun.* **1994**, 801-802.
- [107] Brown, K. R.; Walter, D. G.; Natan, M. J. Seeding of Colloidal Au Nanoparticle Solutions. 2. Improved Control of Particle Size and Shape; *Chem. Mater.* **2000**, *12*, 306-313.
- [108] Goia, D. V.; Matijevic, E. Tailoring the Particle Size of Monodispersed Colloidal Gold; *Colloids Surf., A* **1999**, *146*, 139-152.
- [109] de la Fuente, J. M.; Alcantara, D.; Penadés, S. Cell Response to Magnetic Glyconanoparticles: Does the Carbohydrate Matter?; *IEEE Trans. Nanobioscience* **2007**, *6*, 275-281.
- [110] Halkes, K. M.; Carvalho de Souza, A.; Elizabeth, C.; Maliaars, P.; Gerwig, G. J.; Kamerling, J. P. A Facile Method for the Preparation of Gold Glyconanoparticles from Free Oligosaccharides and Their Applicability in Carbohydrate-protein Interaction Studies; *Eur. J. Org. Chem.* **2005**, 3650-3659.
- [111] Svarovsky, S. A.; Szekely, Z.; Barchi, J. J. Synthesis of Gold Nanoparticles Bearing the Thomsen-Friedenreich Disaccharide: a New Multivalent Presentation of an Important Tumor Antigen; *Tetrahedron Asymm.* **2005**, *16*, 587-598.
- [112] Chen, Y.-J.; Chen, S.-H.; Chien, Y.-Y.; Chang, Y.-W.; Liao, H.-K.; Chang, C.-Y.; Jan, M.-D.; Wang, K.-T.; Lin, C.-C. Carbohydrate-encapsulated Gold Nanoparticles for Rapid Target-protein Identification and Binding-epitope Mapping; *ChemBioChem* **2005**, *6*, 1169-1173.
- [113] Nolting, B.; Yu, J.-J.; Liu, G.-Y.; Cho, S.-J.; Kaulzarich, S.; Gervay-Hague, J. Synthesis of Gold Glyconanoparticles and Biological Evaluation of Recombinant gp120 Interactions; *Langmuir* **2003**, *19*, 6465-6473.
- [114] de la Fuente, J. M.; Barrientos, A. G.; Rojas, T. C.; Rojo, J.; Canada, J.; Fernandez, A.; Penadés, S. Gold Glyconanoparticles as Water-soluble Polyvalent Models to Study Carbohydrate Interactions; *Angew. Chem. Int. Ed.* **2001**, *40*, 2257-2261.
- [115] Sundgren, A.; Barchi, J. J. Varied Presentation of the Thomsen-Friedenreich Disaccharide Tumor-associated Carbohydrate Antigen on Gold Nanoparticles; *Carbohydr. Res.* **2008**, *343*, 1594-1604.
- [116] Mahon, E.; Aastrup, T.; Barboiu, M. Multivalent Recognition of Lectins by Glyconanoparticle Systems; *Chem. Commun.* **2010**, 5491-5493.
- [117] Thygesen, M. B.; Sørensen, K. K.; Clø, E.; Jensen, K. J. Direct Chemoselective Synthesis of Glyconanoparticles from Unprotected Reducing Glycans and Glycopeptide Aldehydes; *Chem. Commun.* **2009**, 6367-6369.
- [118] Thygesen, M. B.; Sauer, J.; Jensen, K. J. Chemoselective Capture of Glycans for Analysis on Gold Nanoparticles: Carbohydrate Oxime Tautomers Provide Functional Recognition by Proteins; *Chem. Eur. J.* **2009**, *15*, 1649 - 1660.
- [119] Chien, Y.-Y.; Jan, M.-D.; Adak, A. K.; Tzeng, H.-C.; Lin, Y.-P.; Chen, Y.-J.; Wang, K.-T.; Chen, C.-T.; Chen, C.-C.; Lin, C.-C. Globotriose-functionalized Gold Nanoparticles as Multivalent Probes for Shiga-like Toxin; *ChemBioChem* **2008**, *9*, 1100-1109.
- [120] Hone, D. C.; Haines, A. H.; Russell, D. A. Rapid, Quantitative Colorimetric Detection of a Lectin Using Mannose-Stabilized Gold Nanoparticles; *Langmuir* **2003**, *19*, 7141-7144.
- [121] Kemp, M. M.; Kumar, A.; Mousa, S.; Dyskin, E.; Yalcin, M.; Ajayan, P.; Linhardt, R. J.; Mousa, S. A. Gold and Silver Nanoparticles Conjugated with Heparin Derivative Possess Anti-angiogenesis Properties; *Nanotech.* **2009**, *20*, 455104.
- [122] Guo, Y.; Yan, H. Preparation and Characterization of Heparin-Stabilized Gold Nanoparticles; *J. Carbohydr. Chem.* **2008**, *27*, 309-319.
- [123] Tromas, C.; Rojo, J.; de la Fuente, J. M.; Barrientos, A. G.; Garcia, R.; Penadés, S. Adhesion forces between Lewis^x determinant antigens as measured by atomic force microscopy; *Angew. Chem. Int. Ed.* **2001**, *40*, 3052-3055.
- [124] de la Fuente, J. M.; Eaton, P.; Barrientos, A. G.; Menendez, M.; Penadés, S. Thermodynamic Evidence for Ca²⁺-Mediated Self-Aggregation of Lewis^x Gold Glyconanoparticles. A Model for Cell Adhesion via Carbohydrate-Carbohydrate Interaction; *J. Am. Chem. Soc.* **2005**, *127*, 6192-6197.
- [125] Hernaiz, M. J.; de la Fuente, J. M.; Barrientos, A. G.; Penadés, S. A Model System Mimicking Glycosphingolipid Clusters to Quantify Carbohydrate Self-interactions by Surface Plasmon Resonance; *Angew. Chem. Int. Ed.* **2002**, *41*, 1554-1557.
- [126] de Souza, A. C.; Halkes, K. M.; Meeldijk, J. D.; Verkleij, A. J.; Vliegthart, J. F. G.; Kamerling, J. P. Gold Glyconanoparticles as Probes to Explore the Carbohydrate-mediated Self-recognition of Marine Sponge Cells; *ChemBioChem* **2005**, *6*, 828-831.
- [127] Lin, C.-C.; Yeh, Y.-C.; Yang, C.-Y.; Chen, G.-F.; Chen, Y.-C.; Wu, Y.-C.; Chen, C.-C. Quantitative Analysis of Multivalent Interactions of Carbohydrate-encapsulated Gold Nanoparticles with Concanavalin A; *Chem. Commun.* **2003**, 2920-2921.
- [128] Liang, C.-H.; Wang, C.-C.; Lin, Y.-C.; Chen, C.-H.; Wong, C.-H.; Wu, C.-Y. Iron Oxide/Gold Core/Shell Nanoparticles for Ultrasensitive Detection of Carbohydrate-Protein Interactions; *Anal. Chem.* **2009**, *81*, 7750-7756.
- [129] Schofield, C. L.; Haines, A. H.; Field, R. A.; Russell, D. A. Silver and Gold Glyconanoparticles for Colorimetric Bioassays; *Langmuir* **2006**, *22*, 6707-6711.
- [130] Sato, Y.; Murakami, T.; Yoshioka, K.; Niwa, O. 12-Mercaptododecyl β -Maltoside-modified Gold Nanoparticles: Specific Ligands for Concanavalin A Having Long Flexible Hydrocarbon Chains *Anal. Bioanal. Chem.* **2008**, *391*, 2527-2532.
- [131] Springer, G. F. Immunoreactive T and Tn epitopes in cancer diagnosis, prognosis, and immunotherapy; *J. Mol. Med.* **1997**, *75*, 594-602.
- [132] de la Fuente, J. M.; Alcantara, D.; Eaton, P.; Crespo, P.; Rojas, T. C.; Fernandez, A.; Hernando, A.; Penadés, S. Gold and Gold-Iron Oxide Magnetic Glyconanoparticles: Synthesis, Characterization and Magnetic Properties; *J. Phys. Chem. B* **2006**, *110*, 13021-13028.
- [133] Martínez-Avila, O.; Hijazi, K.; Marradi, M.; Clavel, C.; Campion, C.; Kelly, C.; Penadés, S. Gold Manno-glyconanoparticles: Multivalent Systems to Block HIV-1 gp120 Binding to the Lectin DC-SIGN; *Chem. Eur. J.* **2009**, *15*, 9874-9888.
- [134] Feinberg, H.; Mitchell, D. A.; Drickamer, K.; Weis, W. I. Structural Basis for Selective Recognition of Oligosaccharides by DC-SIGN and DC-SIGNR; *Science* **2001**, *294*, 2163-2166.
- [135] Martínez-Avila, O.; Bedoya, L. M.; Marradi, M.; Clavel, C.; Alcamí, J.; Penadés, S. Multivalent Manno-Glyconanoparticles Inhibit DC-SIGN-Mediated HIV-1 Trans-Infection of Human T Cells; *ChemBioChem* **2009**, *10*, 1806-1809.
- [136] Lin, C. C.; Yeh, Y. C.; Yang, C. Y.; Chen, C. L.; Chen, G. F.; Chen, C. C.; Wu, Y. C. Selective Binding of Mannose-Encapsulated Gold Nanoparticles to Type 1 Pili in *Escherichia coli*; *J. Am. Chem. Soc.* **2002**, *124*, 3508-3509.
- [137] Schofield, C. L.; Field, R. A.; Russell, D. A. Glyconanoparticles for the Colorimetric Detection of Cholera Toxin; *Anal. Chem.* **2007**, *79*, 1356-1361 and references cited therein.
- [138] Nath, S.; Kaittanis, C.; Tinkham, A.; Perez, J. M. Dextran-Coated Gold Nanoparticles for the Assessment of Antimicrobial Susceptibility; *Anal. Chem.* **2008**, *80*, 1033-1038.
- [139] Ahmed, M.; Deng, Z.; Liu, S.; Lafrenie, R.; Kumar, A.; Narain, R. Cationic Glyconanoparticles: Their Complexation with DNA, Cellular Uptake, and Transfection Efficiencies; *Bioconjugate Chem.* **2009**, *20*, 2169-2176.
- [140] Eaton, P.; Ragusa, A.; Clavel, C.; Rojas Cristina, T.; Graham, P.; Duran Raul, V.; Penadés, S. Glyconanoparticle-DNA interactions: an atomic force microscopy study; *IEEE Trans Nanobioscience* **2007**, *6*, 309-18.
- [141] de la Fuente, M.; Seijo, B.; Alonso, M. J. Novel Hyaluronic Acid-Chitosan Nanoparticles for Ocular Gene Therapy; *Invest. Ophthalmol. Vis. Sci.* **2008**, *49*, 2016-24.
- [142] de la Fuente, M.; Seijo, B.; Alonso, M. J. Bioadhesive Hyaluronan-chitosan Nanoparticles can Transport Genes Across the Ocular Mucosa and Transfect Ocular Tissue; *Gene Ther.* **2008**, *15*, 668-676.
- [143] Lee, H.; Lee, K.; Kim, I. K.; Park, T. G. Synthesis, Characterization, and *in vivo* Diagnostic Applications of Hyaluronic Acid Immobilized Gold Nanoparticles; *Biomaterials* **2008**, *29*, 4709-4718.
- [144] Marradi, M.; Alcantara, D.; de la Fuente, J. M.; Garcia-Martin, M. L.; Cerdan, S.; Penadés, S. Paramagnetic Gd-based Gold Glyconanoparticles as Probes for MRI: Tuning Relaxivities with Sugars; *Chem. Commun.* **2009**, 3922-3924.
- [145] Rojo, J.; Diaz, V.; de la Fuente, J. M.; Segura, I.; Barrientos, A. G.; Riese, H. H.; Bernad, A.; Penadés, S. Gold Glyconanoparticles as New Tools in Antiadhesive Therapy; *ChemBioChem* **2004**, *5*, 291-297.

- [146] Wang, Z.; Xu, Y.; Yang, B.; Tiruchinapally, G.; Sun, B.; Liu, R.; Dulaney, S.; Liu, J.; Huang, X. Preactivation-Based, One-Pot Combinatorial Synthesis of Heparin-like Hexasaccharides for the Analysis of Heparin-Protein Interactions; *Chem. Eur. J.* **2010**, *16*, 8365-8375 and references cited therein.
- [147] Chan, W. C. W.; Nie, S. Quantum Dot Bioconjugates for Ultrasensitive Nonisotopic Detection; *Science* **1998**, *281*, 2016-2018.
- [148] Kikkeri, R.; Lepenies, B.; Adibekian, A.; Laurino, P.; Seeberger, P. H. *In vitro* Imaging and *in vivo* Liver Targeting with Carbohydrate Capped Quantum Dots; *J. Am. Chem. Soc.* **2009**, *131*, 2110-2112.
- [149] Bhang, S. H.; Won, N.; Lee, T.-J.; Jin, H.; Nam, J.; Park, J.; Chung, H.; Park, H.-S.; Sung, Y.-E.; Hahn, S. K.; Kim, B.-S.; Kim, S. Hyaluronic Acid-Quantum Dot Conjugates for *in vivo* Lymphatic Vessel Imaging; *ACS Nano* **2009**, *3*, 1389-1398.
- [150] Jiang, X.; Ahmed, M.; Deng, Z.; Narain, R. Biotinylated Glyco-functionalized Quantum Dots: Synthesis, Characterization, and Cytotoxicity Studies; *Bioconjugate Chem.* **2009**, *20*, 994-1001.
- [151] Babu, P.; Sinha, S.; Suroliya, A. Sugar-Quantum Dot Conjugates for a Selective and Sensitive Detection of Lectins; *Bioconjugate Chem.* **2007**, *18*, 146-151.
- [152] Svarovsky, S. A.; Barchi, J. J., Jr. De novo Synthesis of Biofunctional Carbohydrate-encapsulated Quantum Dots; Demchenko, A. V., Ed., Ed.; Oxford University Press: New York, NY, **2007**, p 375-394.
- [153] Oh, E.; Lee, D.; Kim, Y.-P.; Cha, S. Y.; Oh, D.-B.; Kang, H. A.; Kim, J.; Kim, H.-S. Nanoparticle-based Energy Transfer for Rapid and Simple Detection of Protein Glycosylation; *Angew. Chem. Int. Ed.* **2006**, *45*, 7959-7963.
- [154] de la Fuente, J. M.; Penadés, S. Glyco-quantum Dots: a New Luminescent System with Multivalent Carbohydrate Display; *Tetrahedron Asymm.* **2005**, *16*, 387-391.
- [155] Robinson, A.; Fang, J.-M.; Chou, P.-T.; Liao, K.-W.; Chu, R.-M.; Lee, S.-J. Probing Lectin and Sperm with Carbohydrate-modified Quantum Dots; *ChemBioChem* **2005**, *6*, 1899-1905.
- [156] Sun, X.-L.; Cui, W.; Haller, C.; Chaikof, E. L. Site-specific Multivalent Carbohydrate Labeling of Quantum Dots and Magnetic Beads; *ChemBioChem* **2004**, *5*, 1593-1596.
- [157] Mukhopadhyay, B.; Martins, M.; Karamanska, R.; Russell, D. A.; Field, R. A. Bacterial Detection Using Carbohydrate-functionalised CdS Quantum Dots: a Model Study Exploiting *E. coli* Recognition of Mannosides; *Tetrahedron Lett.* **2009**, *50*, 886-889.
- [158] Osaki, F.; Kanamori, T.; Sando, S.; Sera, T.; Aoyama, Y. A Quantum Dot Conjugated Sugar Ball and Its Cellular Uptake. On the Size Effects of Endocytosis in the Subviral Region; *J. Am. Chem. Soc.* **2004**, *126*, 6520-6521.
- [159] Kim, K.; Hur, W.; Park, S.-J.; Hong, S. W.; Choi, J. E.; Goh, E. J.; Yoong, S. K.; Hahn, S. K. Bioimaging for Targeted Delivery of Hyaluronic Acid Derivatives to the Livers in Cirrhotic Mice Using Quantum Dots; *ACS Nano* **2010**, *4*, 3005-3014.
- [160] Kikkeri, R.; Laurino, P.; Odedra, A.; Seeberger, P. H. Synthesis of Carbohydrate-functionalized Quantum Dots in Microreactors; *Angew. Chem. Int. Ed.* **2010**, *49*, 2054-2057.
- [161] Wu, P.; Chen, X.; Hu, N.; Tam, U. C.; Blixt, O.; Zettl, A.; Bertozzi, C. R. Biocompatible Carbon Nanotubes Generated by Functionalization with Glycodendrimers; *Angew. Chem. Int. Ed.* **2008**, *47*, 5022-5025.
- [162] Chen, X.; Tam, U. C.; Czapinski, J. L.; Lee, G. S.; Rabuka, D.; Zettl, A.; Bertozzi, C. R. Interfacing Carbon Nanotubes with Living Cells; *J. Am. Chem. Soc.* **2006**, *128*, 6292-6293.
- [163] Chen, X.; Lee, G. S.; Zettl, A.; Bertozzi, C. R. Biomimetic Synthesis: Biomimetic Engineering of Carbon Nanotubes by Using Cell Surface Mucin Mimics; *Angew. Chem. Int. Ed.* **2004**, *43*, 6111-6116.
- [164] Gu, L.; Luo, P.; Wang, H.; Mezziani, M. J.; Lin, Y.-S.; Veca, L. M.; Cao, L.; Lu, F.; Wang, X.; Quinn, R. A.; Wang, W.; Zhang, P.; Lacher, S.; Sun, Y.-P. Single-Walled Carbon Nanotube as a Unique Scaffold for the Multivalent Display of Sugars; *Biomacromolecules* **2008**, *9*, 2408-2418.
- [165] Gu, L.; Elkin, T.; Jiang, X.; Li, H.; Lin, Y.; Qu, L.; Tzeng, T. R. J.; Joseph, R.; Sun, Y. P. Single-walled Carbon Nanotubes Displaying Multivalent Ligands for Capturing Pathogens; *Chem. Commun.* **2005**, 874-876.
- [166] Luo, P. G.; Wang, H.; Gu, L.; Lu, F.; Lin, Y.; Christensen, K. A.; Yang, S.-T.; Sun, Y.-P. Selective Interactions of Sugar-Functionalized Single-Walled Carbon Nanotubes with Bacillus Spores; *ACS Nano* **2009**, *3*, 3909-3916.
- [167] Wang, H.; Gu, L.; Lin, Y.; Lu, F.; Mezziani, M. J.; Luo, P. G.; Wang, W.; Cao, L.; Sun, Y. P. Unique Aggregation of Anthrax (*Bacillus anthracis*) Spores by Sugar-Coated Single-Walled Carbon Nanotubes; *J. Am. Chem. Soc.* **2006**, *128*, 13364-13365.
- [168] Astruc, D.; Boisselier, E.; Ornelas, C. Dendrimers Designed for Functions: From Physical, Photophysical, and Supramolecular Properties to Applications in Sensing, Catalysis, Molecular Electronics, Photonics, and Nanomedicine; *Chem. Rev.* **2010**, *110*, 1857-1959.
- [169] Bosman, A. W.; Janssen, H. M.; Meijer, E. W. About Dendrimers: Structure, Physical Properties, and Applications; *Chem. Rev.* **1999**, *99*, 1665-1688.
- [170] Turnbull, W. B.; Stoddart, J. F. Design and Synthesis of Glycodendrimers; *Rev. Mol. Biotechnol.* **2002**, *90*, 231-255.
- [171] Roy, R. Glycodendrimers. A new class of biopolymers; *Polym. News* **1996**, *21*, 226-232.
- [172] Page, D.; Zanini, D.; Roy, R. Macromolecular Recognition: Effect of Multivalency in the Inhibition of Binding of Yeast Mannan to Concanavalin A and Pea Lectins by Mannosylated Dendrimers; *Bioorg. Med. Chem.* **1996**, *4*, 1949-1961.
- [173] Andre, S.; Pieters, R. J.; Vrasidas, I.; Kaltner, H.; Kuwabara, I.; Liu, F.-T.; Liskamp, R. M. J.; Gabius, H.-J. Wedgelike Glycodendrimers as Inhibitors of Binding of Mammalian Galectins to Glycoproteins, Lactose Maxicusters, and Cell Surface Glycoconjugates; *ChemBioChem* **2001**, *2*, 822-830.
- [174] Pieters, R. J. Maximizing Multivalency Effects in Protein-carbohydrate Interactions; *Org. Biomol. Chem.* **2009**, *7*, 2013-2025.
- [175] Pieters, R. J.; Liskamp, R. M. J. Multivalent Presentation Strategies in Novel Inhibitors of Bacterial (toxin) Adhesion and Synthetic Vaccines; *Anti-Infect. Agents Med. Chem.* **2008**, *7*, 193-200.
- [176] Sisu, C.; Baron, A. J.; Branderhorst, H. M.; Connell, S. D.; Weijers, C. A. G. M.; de Vries, R.; Hayes, E. D.; Pukin, A. V.; Gilbert, M.; Pieters, R. J.; Zuilhof, H.; Visser, G. M.; Turnbull, W. B. The Influence of Ligand Valency on Aggregation Mechanisms for Inhibiting Bacterial Toxins; *ChemBioChem* **2009**, *10*, 329-337.
- [177] Deguise, I.; Lagnoux, D.; Roy, R. Synthesis of Glycodendrimers Containing Both Fucoside and Galactoside Residues and Their Binding Properties to PA-IL and PA-III Lectins from *Pseudomonas aeruginosa*; *New J. Chem.* **2007**, *31*, 1321-1331.
- [178] Touaibia, M.; Wellens, A.; Shiao, T. C.; Wang, Q.; Sirois, S.; Bouckaert, J.; Roy, R. Mannosylated G(0) Dendrimers with Nano-molar Affinities to *Escherichia coli* FimH; *ChemMedChem* **2007**, *2*, 1190-1201.
- [179] Schlick, K. H.; Udelhoven, R. A.; Strohmeyer, G. C.; Cloninger, M. J. Binding of Mannose-functionalized Dendrimers with Pea (*Pisum sativum*) Lectin; *Mol. Pharm.* **2005**, *2*, 295-301.
- [180] Mangold, S. L.; Morgan, J. R.; Strohmeyer, G. C.; Gronenborn, A. M.; Cloninger, M. J. Cyanovirin-N Binding to Man1-2Man Functionalized Dendrimers; *Org. Biomol. Chem.* **2005**, *3*, 2354-2358.
- [181] Wolfenden, M. L.; Cloninger, M. J. Mannose/glucose-functionalized Dendrimers to Investigate the Predictable Tunability of Multivalent Interactions; *J. Am. Chem. Soc.* **2005**, *127*, 12168-12169 and references therein.
- [182] Wolfenden, M. L.; Cloninger, M. J. Carbohydrate-functionalized Dendrimers to Investigate the Predictable Tunability of Multivalent Interactions; *Bioconjugate Chem.* **2006**, *17*, 958-966 and references therein.
- [183] Woller, E. K.; Walter, E. D.; Morgan, J. R.; Singel, D. J.; Cloninger, M. J. Altering the Strength of Lectin Binding Interactions and Controlling the Amount of Lectin Clustering Using Mannose/hydroxyl-functionalized Dendrimers; *J. Am. Chem. Soc.* **2003**, *125*, 8820-8826.
- [184] Woller, E. K.; Cloninger, M. J. The Lectin-binding Properties of Six Generations of Mannose-functionalized Dendrimers; *Org. Lett.* **2002**, *4*, 7-10.
- [185] Seah, N.; Santacroce, P. V.; Basu, A. Probing the Lactose-GM3 Carbohydrate-Carbohydrate Interaction with Glycodendrimers; *Org. Lett.* **2009**, *11*, 559-562.
- [186] Mak, R. H.; Kuo, H.-J. Pathogenesis of Urinary Tract Infection: an Update; *Curr. Opin. Pediatr.* **2006**, *18*, 148-52.
- [187] Palmer, L. M.; Reilly, T. J.; Utsalo, S. J.; Donnenberg, M. S. Internalization of *Escherichia coli* by Human Renal Epithelial Cells is Associated with Tyrosine Phosphorylation of Specific Host Cell Proteins; *Infect. Immun.* **1997**, *65*, 2570-2575.
- [188] Sharon, N. Carbohydrates as Future Anti-adhesion Drugs for Infectious Diseases; *Biochim. Biophys. Acta* **2006**, *1760*, 527-537.
- [189] Wellens, A.; Garofalo, C.; Nguyen, H.; van Gerven, N.; Slattegard, R.; Hernalsteens, J.-P.; Wyns, L.; Oscarson, S.; de Greve, H.; Hultgren, S.; Bouckaert, J. Intervening with Urinary Tract Infections Using Anti-adhesives Based on the Crystal Structure of the FimH-oligomannose-3 Complex; *PLoS One* **2008**, *3*, 4.
- [190] Choudhury, D.; Thompson, A.; Stojanoff, V.; Langermann, S.; Pinkner, J.; Hultgren, S. J.; Knight, S. D. X-ray Structure of the FimC-FimH Chaperone-adhesin Complex from Uropathogenic *Escherichia coli*; *Science* **1999**, *285*, 1061-1066.
- [191] Firon, N.; Ofek, I.; Sharon, N. Interaction of Mannose-containing Oligosaccharides with the Fimbrial Lectin of *Escherichia coli*; *Biochem. Biophys. Res. Commun.* **1982**, *105*, 1426-1432.
- [192] Firon, N.; Ashkenazi, S.; Mirelman, D.; Ofek, I.; Sharon, N. Aromatic Alpha-glycosides of Mannose are Powerful Inhibitors of the Adherence of Type 1 Fimbriated *Escherichia coli* to Yeast and Intestinal Epithelial Cells; *Infect. Immun.* **1987**, *55*, 472-476.
- [193] Nagahori, N.; Lee, R. T.; Nishimura, S.-I.; Page, D.; Roy, R.; Lee, Y. C. Inhibition of Adhesion of Type 1 Fimbriated *Escherichia coli* to Highly Mannosylated Ligands; *ChemBioChem* **2002**, *3*, 836-844.
- [194] Salminen, A.; Loimaranta, V.; Joosten, J. A. F.; Khan, A. S.; Hacker, J.; Pieters, R. J.; Finne, J. Inhibition of P-fimbriated *Escherichia coli* Adhesion by Multivalent Galabiose Derivatives Studied by a Live-bacteria Application of Surface Plasmon Resonance; *J. Antimicrob. Chemother.* **2007**, *60*, 495-501.
- [195] Branderhorst, H. M.; Kooij, R.; Salminen, A.; Jongeneel, L. H.; Arnusch, C. J.; Liskamp, R. M. J.; Finne, J.; Pieters, R. J. Synthesis of Multivalent *Streptococcus suis* Adhesion Inhibitors by Enzymatic Cleavage of Polygalacturonic Acid and 'Click' Conjugation; *Org. Biomol. Chem.* **2008**, *6*, 1425-1434.
- [196] Joosten, J. A. F.; Loimaranta, V.; Appeldoorn, C. C. M.; Haataja, S.; El Maate, F. A.; Liskamp, R. M. J.; Finne, J.; Pieters, R. J. Inhibition of

- Streptococcus suis Adhesion by Dendritic Galabiose Compounds at Low Nanomolar Concentration; *J. Med. Chem.* **2004**, *47*, 6499-6508.
- [197] Hansen, H. C.; Haataja, S.; Finne, J.; Magnusson, G. Di-, Tri-, and Tetraivalent Dendritic Galabiosides that Inhibit Hemagglutination by Streptococcus suis at Nanomolar Concentration; *J. Am. Chem. Soc.* **1997**, *119*, 6974-6979.
- [198] Rojo, J.; Delgado, R. Glycodendritic Structures: Promising New Antiviral Drugs; *J. Antimicrob. Chemother.* **2004**, *54*, 579-581.
- [199] Lasala, F.; Arce, E.; Otero, J. R.; Rojo, J.; Delgado, R. Mannosyl Glycodendritic Structure Inhibits DC-SIGN-Mediated Ebola Virus Infection in cis and in trans; *Antimicrob. Agents Chemother.* **2003**, *47*, 3970-3972.
- [200] Roy, R.; Baek, M.-G.; Rittenhouse-Olson, K. Synthesis of N,N ϵ -bis(Acrylamido)acetic Acid-Based T-Antigen Glycodendrimers and Their Mouse Monoclonal IgG Antibody Binding Properties; *J. Am. Chem. Soc.* **2001**, *123*, 1809-1816.
- [201] Thoma, G.; Streiff, M. B.; Katopodis, A. G.; Duthaler, R. O.; Voelcker, N. H.; Ehrhardt, C.; Masson, C. Non-Covalent Polyvalent Ligands by Self-Assembly of Small Glycodendrimers: A Novel Concept for the Inhibition of Polyvalent Carbohydrate-Protein Interactions *In vitro* and *In vivo*; *Chem. Eur. J.* **2006**, *12*, 99-117.
- [202] Thoma, G.; Katopodis, A. G.; Voelcker, N. H.; Duthaler, R. O.; Streiff, M. B. Novel Glycodendrimers Self-Assemble to Nanoparticles which Function as Polyvalent Ligands *In vitro* and *In vivo*; *Angew. Chem. Int. Ed.* **2002**, *41*, 3195-3198.
- [203] Shaunak, S.; Thomas, S.; Gianasi, E.; Godwin, A.; Jones, E.; Teo, I.; Mireskandari, K.; Luthert, P.; Duncan, R.; Patterson, S.; Khaw, P.; Brocchini, S. Polyvalent Dendrimer Glucosamine Conjugates Prevent Scar Tissue Formation; *Nature Biotech.* **2004**, *22*, 977-984.
- [204] Krist, P.; Herkommerová -Rajnochová, E.; Rauvolfová, J.; Semeňuk, T.; Vavrušková, P.; Pavlíček, J.; Bezouška, K.; Petruš, L.; Krěn, V. Toward an Optimal Oligosaccharide Ligand for Rat Natural Killer Cell Activation Receptor NKR-P1; *Biochem. Biophys. Res. Commun.* **2001**, *287*, 11-20.
- [205] Krist, P.; Vannucci, L.; Kuzma, M.; Man, P.; Sadalapure, K.; Patel, A.; Bezouška, K.; Pospíšil, M.; Petruš, L.; Lindhorst, T. K.; Krěn, V. Fluorescent Labelled Thiourea-Bridged Glycodendrons; *ChemBioChem* **2001**, *5*, 445-452.
- [206] Bezouška, K.; Krěn, V.; Kieburg, C.; Lindhorst, T. K. GlcNAc-terminated Glycodendrimers Form Defined Precipitates with the Soluble Dimeric Receptor of Rat Natural Killer Cells, sNKR-P1A; *FEBS Lett.* **1998**, *426*, 243-247.
- [207] Vannucci, L.; Fiserová, A.; Sadalapure, K.; Lindhorst, T. K.; Kuldová, M.; Rossmann, P.; Horváth, O.; Krěn, V.; Krist, P.; Bezouška, K.; Luptovcová, M.; Mosca, F.; Pospíšil, M.; Krěn, V. Effects of N-acetyl-glucosamine-coated Glycodendrimers as Biological Modulators in the B16F10 Melanoma Model *in vivo*; *Int. J. Oncol.* **2003**, *23*, 285-296.
- [208] Hulikova, K.; Benson, V.; Svoboda, J.; Sima, P.; Fiserova, A. N-Acetyl-D-glucosamine-coated Polyamidoamine Dendrimer Modulates Antibody Formation *via* Natural Killer Cell Activation; *Int. Immunopharmacol.* **2009**, *9*, 792-799.

Received: January 04, 2011

Revised: April 03, 2011

Accepted: April 04, 2011